Eberhard Karls Universität Tübingen
Faculty of Mathematics and Natural Sciences
Cognitive Neuroscience

Bachelor's Thesis in Cognitive Science

Parsimonious Procedures for the Combination of Odometry and Landmark Information in Path Integration

Daniela Winter

March 10, 2021

Referee

Prof. Dr. Hanspeter A. Mallot
Cognitive Neuroscience
University of Tübingen

Supervisors

Prof. Dr. Hanspeter A. Mallot
Tristan Baumann
Cognitive Neuroscience
University of Tübingen

Winter, Daniela
Parsimonious Procedures for the Combination of Odometry and Landmark Information in Path Integration
Bachelor's Thesis in Cognitive Science
University of Tübingen

Contents

1 Abstract

In this work, different types of path integration are compared according to their robustness against errors. Idiothetic as well as allothetic path integration is considered. During idiothetic path integration, an agent has only access to proprioceptive information such as kinetic and vestibular perception. For allothetic path integration, only one landmark is available to the agent at a time, which severely restricts the information accessible through the environment.
If the landmark is at a sufficient distance, error robust path integration is possible without knowing the position of the landmark. If the landmark is close, the position of the landmark can be estimated by combining idio- and allothetic information with little additional computational effort. Path integration with known landmark position proves to be the most error robust model of the ones that are evaluated in this work.
It therefore seems reasonable to consider path integration where both idiothetic and allothetic information is available in studies about spatial orientation. So far, this has largely been studied separately. However, this separation seems rather arbitrary as this work shows that the underlying procedure is very similar.

2 Motivation

Path integration is an important principle of spatial orientation. It describes the ability to continuously determine one's own position. In path integration, each new position of an agent is calculated based on the previous one. This is done using information about the distance of movement and information about the direction of movement, which is the current heading. If an agent knows its position relative to an initial position and knows the current heading, it also has the necessary information to be able to find its initial position.
From an evolutionary point of view, the ability to return to a certain position plays a crucial role. With the help of path integration, an agent can, for example, return to the nest after foraging. This is possible even if the nest is out of sight. This ability is possessed by mammals, insects and birds, among others (Papi, 1992).
Spatial orientation is also an essential ability for mobile robots. Not all environments can be known in advance and provided to the system as maps. GPS data for the detection of its own position is also not always available (Wang et al., 2014). Therefore, it is important to implement spatial orientation procedures (such as path integration) so that the agent can use the available information to find its way in unknown environments.

Typically, path integration is understood as a purely idiothetic path integration. In this case, only proprioceptive movement information is available to the agent. The agent can not use any information from the environment, so-called allothetic information for its localisation. Allothetic information includes visual and auditory information, for example. This idiothetic path integration has been observed in many species, including ants, bees and various mammals (Etienne et al., 1996). Problematically, errors in localisation estimates accumulate over time if purely idiothetic path integration is used (Etienne et al., 1996). Errors that already exist can no longer be compensated for, since no adjustment with the environment takes place.
The study of purely idiothetic path integration, which excludes any allothetic information, is an artificial problem and not very close to reality. This is because in most cases an agent has the ability to perceive its environment. This allothetic information can be used for path integration as well. In reality, path integration works through an interaction of idiothetic proprioception and allothetic environmental information (Anagnostou et al., 2018). With perfect perception, idiothetic and allothetic information is redundant. Under the influence of error factors, however, the additional information could be used to minimise errors.

Following this idea, approaches to investigate path integration where allothetic information is also available to the agent have been developed. In that case, the agent can match its own movement with the direction of a compass, for example. There are many vertebrates, including fish, pigeons and even some mammals, that can use the earth's magnetic field as a compass (Wiltschko & Wiltschko, 2005; Gould, 2008).
But compass information is not always available to every agent. If that is the case, distant landmarks can be used as allothetic information for path integration instead of a compass. One's own movement is then estimated relative to these landmarks. It has been shown that people use distant landmarks for their navigation (Steck & Mallot, 2000). Landmarks that are closer to the agent can also be used for localisation. In robotics, a method called SLAM (simultaneous localisation and mapping) is often applied to mobile robots, which estimate the position of landmarks and use this estimation to determine the position of the agent. It is an iterative, probabilistic method that often involves high computational cost and the trade-off of a lot of sensor information (Urzua et al., 2017; Bailey & Durrant-Whyte, 2006).

In contrast to that, this work investigates methods that mathematically solve the path integration problem with only very limited idiothetic and allothetic information. It is shown which errors occur with the respective types of path integration and how the combination of idiothetic and allothetic path integration leads to a more robust localisation. For this, a simplification to very limited information is made. This has the advantage of providing a parsimonious model which makes it possible to show and investigate the weaknesses of each type of path integration separately.
In reality, the agent has a wide range of information at its disposal that it can use for its orientation. The processing of various types of information in the brain works in a modular way (Velik, 2008). The models discussed here can describe the individual processes. These individual processes executed in a parallel fashion then could simulate the overall performance of the agent.
By combining idio- and allothetic path integration, this work furthermore analyses whether the strict separation between the term of idiothetic path integration and allothetic localisation methods, such as SLAM, spatial updating[1], snapshot homing[2] or the use of optic flow[3], is useful and necessary.

[1]Localisation procedure in which a constant updating of the positions of landmarks in the environment takes place during the agent's own movement (Wolbers et al., 2008).

[2]By comparing a stored snapshot of the destination view and the currently perceived environment, the movement of the agent is calculated with the aim of reducing the existing differences (Cartwright & Collett, 1983).

[3]When using optic flow for orientation, the movement patterns of points in the visual field are used to draw conclusions about one's own movement (Gibson, 1950).

In this work, an extended meaning of the term of path integration is used that includes both, the possibility of idiothetic and allothetic information use. Essentially, path integration is about calculating the current position from the previous position using the current heading and the distance travelled. How the information of heading and distance are obtained can vary. In the following, different types of path integration are studied which differ in the type of information that is used to determine the current heading.

3 Models of Path Integration

In this chapter, the described types of path integration are mathematically modelled so that later, they can be compared with each other in a simulation.

In path integration, the current heading $\hat{\eta}_t$ and the length of the step taken $\hat{\Delta x}_t$ are needed to determine the current position $(\hat{x}_{1,t}|\hat{x}_{2,t})$ relative to the previous position $(\hat{x}_{1,t-1}|\hat{x}_{2,t})$. The current position can then be calculated as follows:

$$\hat{x}_{1,t} = \hat{x}_{1,t-1} + \hat{\Delta x}_t * cos(\hat{\eta}_t) \tag{3.1}$$

$$\hat{x}_{2,t} = \hat{x}_{2,t-1} + \hat{\Delta x}_t * sin(\hat{\eta}_t) \tag{3.2}$$

Values known to the agent are marked with a circumflex. Other values are unknown to the agent. The positions of the agent are stored as Cartesian coordinates geocentric with origin at the starting point of the path.

In reality, locomotion and estimation of the new position are performed continuously. In this simulation, however, discrete steps with fixed lengths $\hat{\Delta x}_t$ are performed. The defined step length is very small (about 1/100 of the total path) so that the simulation resembles a continuous movement as much as possible. The length of each step is fixed and known to the agent so that it only has to calculate the heading $\hat{\eta}_t$. This restriction to rotation measurements without translation measurements means that errors can only occur in the heading. This focus on rotation measurement corresponds to the approach of Klatzky et al. (Klatzky et al., 1998).
In the simulation, a discrete step runs in the following order. First the agent rotates to change its heading. Then, the translational step is performed, followed by the estimation of position.

Under perfect conditions, the formulas always provide the correct heading, resulting in a perfect path estimate. In reality, however, measurements are subject to error, which affects path integration. Therefore, a random error is added to all measurements. The aim is then to test which types of path integration are more prone to this error and which are more robust.
Error noise can affect the measurement in two different ways: With additive noise, the error $\epsilon_{+,t}$ is added to the measured value. Therefore, the variation from the perfect value is absolute. With multiplicative noise, the erroneous value differs from the perfect value by a certain error percentage. The error $\epsilon_{*,t}$ is therefore multiplied by the measurement. The deviation is thus relative and depends on the size of the measured value.

Both types of error occur in reality. Additive errors occur when the agent has a slight jitter in its movement execution. No matter how much the change in movement, the jitter changes the movement by a certain value. Additive errors can also occur when external influences such as an air or water flow unintentionally change the movement. Multiplicative errors can arise in the case of direct misestimations of quantities. For example, with an angle estimate of 270 degrees, it is more likely to misestimate by 20 degrees than with an angle estimate of one degree. Therefore, it makes sense to add a multiplicative error for such cases, which is relative to the size of the measured value.

In the following, the error is only related to measurements of the agent, no calculation or rounding errors are assumed during the application and interpretation of the measured values. Due to the parsimony of the model, the idiothetic and allothetic measurements of the agent are restricted to the following values per step.

ODO: rotational step ($\hat{\Delta\omega}_t$)
COMP: compass bearing ($\hat{\alpha}_t$)
LM_COMP: bearing to landmark ($\hat{\beta}_t$)
LM_OF: change of bearing to landmark ($\hat{\Delta\beta}_t$)
LM_POS: rotational step and bearing to landmark ($\hat{\Delta\omega}_t$, $\hat{\beta}_t$)

These different measurements and the abbreviations are described in detail in the following sections.
When deriving the formula, the four-quadrant arc tangent $arctan2$ is used because, unlike the normal arc tangent, it provides values in the range from $-\pi$ to π instead of $-\pi/2$ to $\pi/2$ and is therefore necessary for calculating all possible angular sizes.

3.1 Idiothetic Path Integration

3.1.1 Odometry (ODO)

Pure idiothetic path integration is based on the approach that an agent has only proprioceptive and no allothetic information available for localisation. This includes kinaesthetic perceptions, which provide information about muscle and joint movement. They also include vestibular perceptions, which provide information about angular accelerations, i.e. rotational movements. Analogously, in vehicle technology and robotics, the use of the system's movement sensors for its own orientation is called *odometry* (Wang et al., 2014). The term of odometry is used in the following synonymously for purely idiothetic path integration without restriction to technical agents.

The actual heading can be calculated from the measured rotational movements by integrating the individual changes of rotation. It can happen that the proprioception of the rotation changes does not correspond to the actual rotation movement performed. This occurs with robots, for example, when the wheels spin on slippery surfaces or sensors are incorrectly calibrated (Kurazume & Hirose, 2000). These measurement errors are contained in each step. The integration of the rotation steps therefore leads to an accumulation of errors (Etienne et al., 1996). The accumulation of errors can not be avoided with purely idiothetic path integration, since no adjustment with the environment is possible.

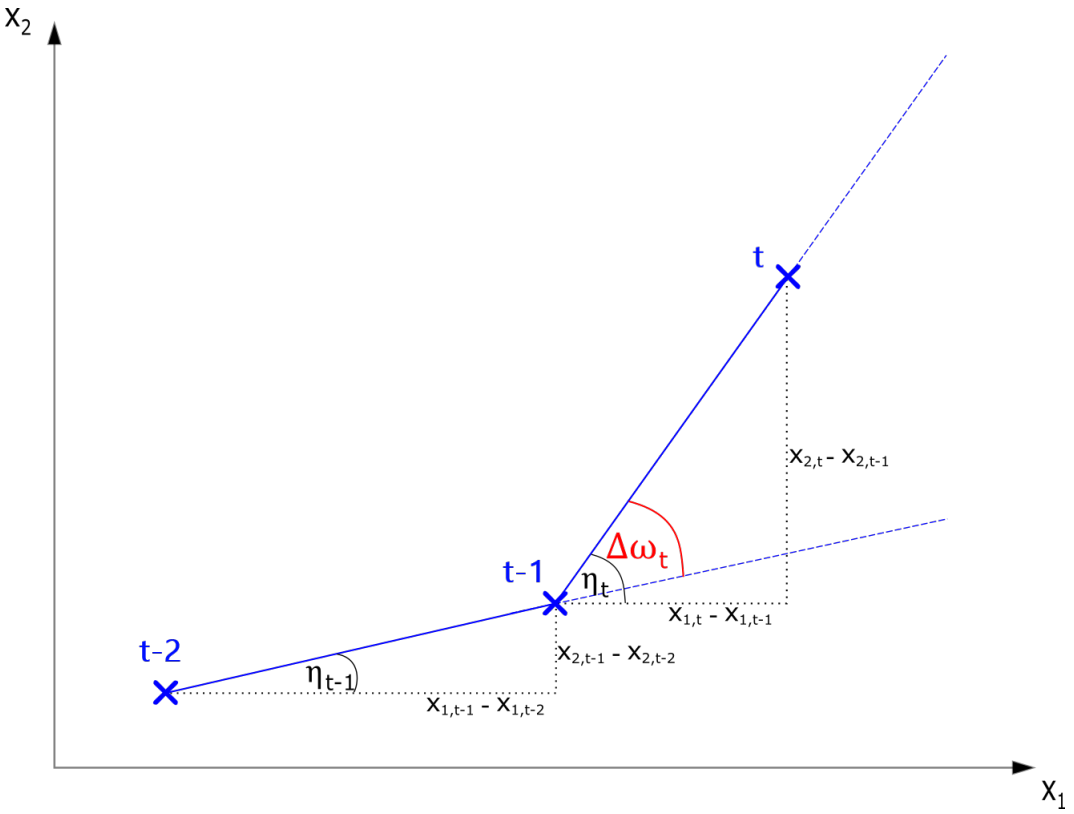

Figure 3.1: Simulation of odometry. The agent walks on a given path and measures the rotational movement $\hat{\Delta\omega}_t$ that takes place between the steps. Crosses show positions of the agent, blue dashed lines show the direction of heading. Measured variables in red.

In figure 3.1 the derivation of the formula for the simulation of odometry is illustrated. The only value the agent measures during each step is the executed change in rotation $\hat{\Delta\omega}_t$. The measurement is simulated by subtracting the true headings of the current η_t and last step η_{t-1} and then adding an additive $\epsilon_{+,t}$ and multiplicative $\epsilon_{*,t}$ error. The headings themselves can be determined

using the arc tangent, since the Cartesian coordinates of the given path and thus the distances in x_1- and x_2-direction are available.

$$\eta_t = arctan2((x_{2,t} - x_{2,t-1}), (x_{1,t} - x_{1,t-1})) \tag{3.3}$$

$$\Delta\omega_t = \eta_t - \eta_{t-1} \tag{3.4}$$

$$\hat{\Delta\omega}_t = \Delta\omega_t * \epsilon_{*,t} + \epsilon_{+,t} \tag{3.5}$$

Using the estimated rotation step $\hat{\Delta\omega}_t$, the agent can determine its heading. This is done by summing up the individual rotation step sizes. With an initial heading of $\hat{\eta}_0 = 0$ (in x_1-axis direction), the summed rotation steps result in the current heading.

$$\hat{\eta}_t = \hat{\eta}_{t-1} + \hat{\Delta\omega}_t \tag{3.6}$$

The summation of the individual $\hat{\Delta\omega}_t$ accumulates the errors contained in $\hat{\Delta\omega}_t$. These can not be corrected in this type of path integration.

3.2 Allothetic Path Integration

3.2.1 Compass Usage (COMP)

One way of using allothetic information is to use a compass. The angle between one's own heading and the compass direction, the so-called bearing $\hat{\alpha}_t$, is measured. The bearing changes directly with the change in the direction of movement. Therefore, the heading can be determined directly from the bearing measurement.
If a compass direction is available, the problem of error accumulation does not exist. The agent measures the angle $\hat{\alpha}_t$ between its current heading and compass direction. Thus, the measurement is not based on the last turning steps, but is reoriented to the compass direction after each step.

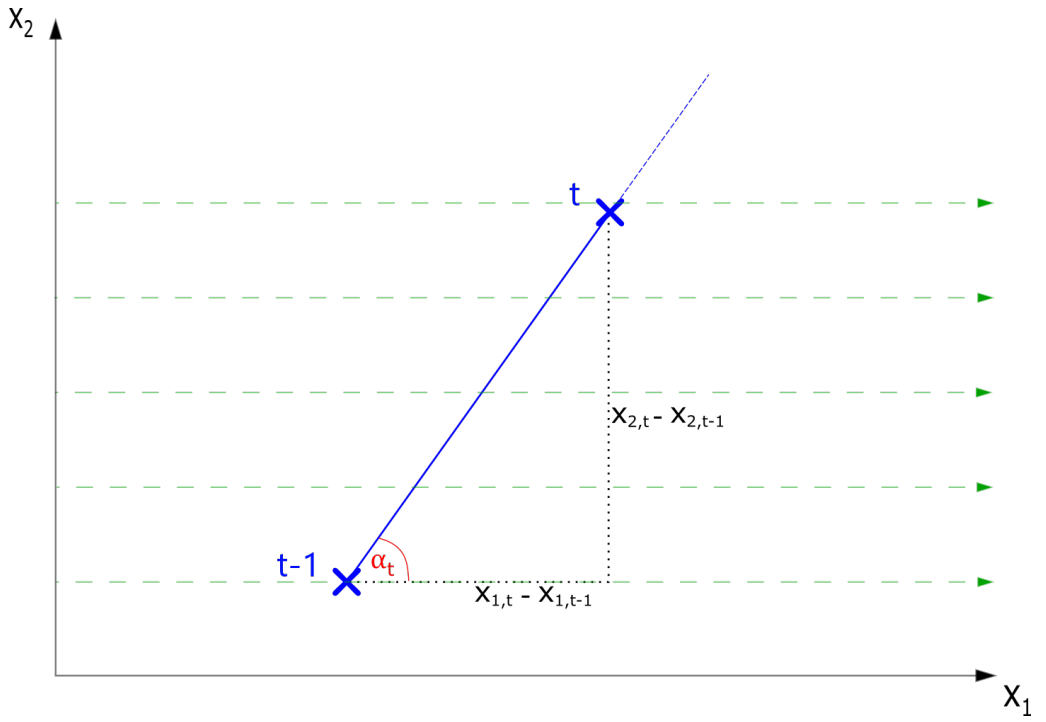

Figure 3.2: Simulation of compass usage. The agent walks on a given path and measures the bearing to the compass direction $\hat{\alpha}_t$, which equals the current heading $\hat{\eta}_t$. Crosses show positions of the agent, blue dashed lines show the direction of heading. Measured variables in red. Compass direction in green.

The following procedure is illustrated in figure 3.2: Without loss of generality, the compass direction can be set in x_1-axis direction. With a starting heading of $\eta_0 = 0$ (in x_1-axis direction), α_0 is zero. The angle of the bearing α_t is the angle between heading η_t and compass direction α_0. In the case of $\alpha_0 = 0$, it therefore corresponds to heading η_t at each step. The angle α_t can be determined using the arc tangent, since the Cartesian coordinates of the positions and thus the distances travelled in x_1- and x_2-directions are known. After adding the additive and multiplicative noise $\epsilon_{+,t}$ and $\epsilon_{*,t}$, the simulated measurement of $\hat{\alpha}_t$ is obtained. With $\hat{\alpha}_0 = 0$ the heading $\hat{\eta}_t$ equals to the compass bearing $\hat{\alpha}_t$.

$$\alpha_t = arctan2((x_{2,t} - x_{2,t-1}), (x_{1,t} - x_{1,t-1})) \tag{3.7}$$

$$\hat{\alpha}_t = \alpha_t * \epsilon_{*,t} + \epsilon_{+,t} \tag{3.8}$$

$$\hat{\eta}_t = \hat{\alpha}_t \tag{3.9}$$

It can be seen that $\hat{\eta}_t$ is calculated in each step directly from the bearing, without dependence on previous values of $\hat{\eta}$. Therefore, there is no accumulation of errors in this type of path integration. The disadvantage is, however, that compass directions are not always available to each agent.

3.2.2 Landmark Usage as Compass (LM_COMP)

In comparison to real compass directions, landmarks are available most of the time. Landmarks are objects in the environment that are used for orientation. The compass direction corresponds to the direction of a landmark which is at an infinite distance. As with a compass, the bearing, i.e. the angle between one's own heading and the direction of the landmark, can be measured. A compass bearing always remains constant, regardless of the agent's position. But as landmarks are not infinitely far away in reality, the bearing to the landmark depends on the position of the agent. The bearing changes not only when the heading changes, but also when the agent's position changes.
Due to the information constraint in this model, the agent has no information about the distance of the landmark and only measures the bearing to the landmark. Therefore, the landmark is assumed to be infinitely far away and hence the landmark direction is interpreted as compass direction. This leads to an error in the estimation of the heading. The error increases the closer the landmark is.

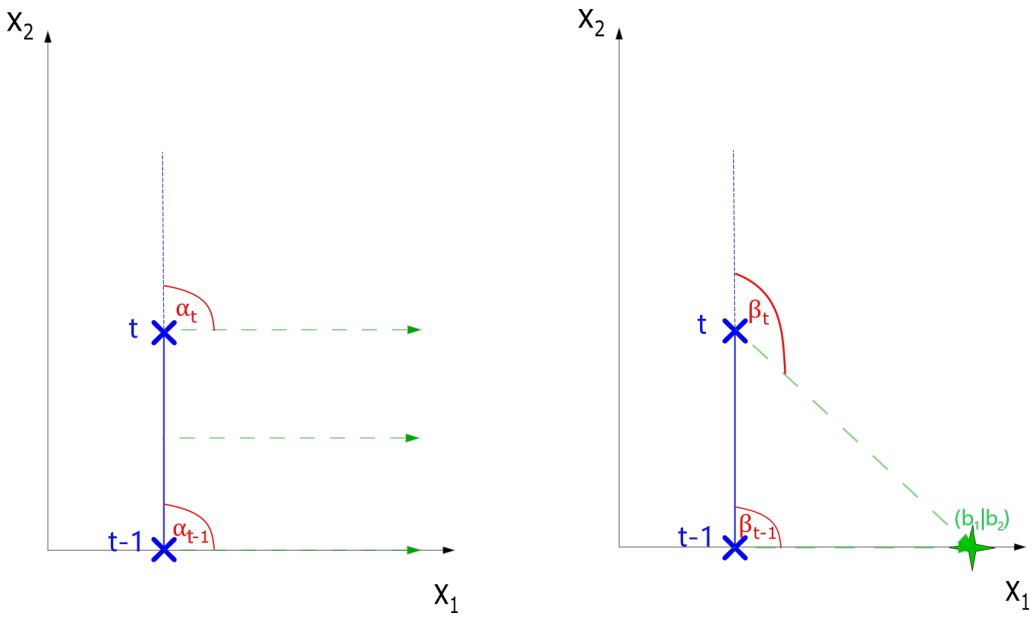

Figure 3.3: Left: Bearing relative to compass direction. The heading of the agent does not change. Therefore, the measured bearings remain the same. **Right**: Bearing relative to landmark at finite distance. The heading of the agent does not change, but the direction of the landmark relative to the agent, and therefore the bearing, changes. Crosses show positions of the agent, blue dashed lines show the direction of heading. Measured variables in red. Compass and landmark direction in green. Landmark position at $(b_1|b_2)$ marked as green star.

The following fact is illustrated in figure 3.3: If a compass or a landmark with infinite distance is used, the bearing does not change if the heading remains the same. However, this is not true if a landmark with finite distance is used. If the heading is constant, the bearing changes.

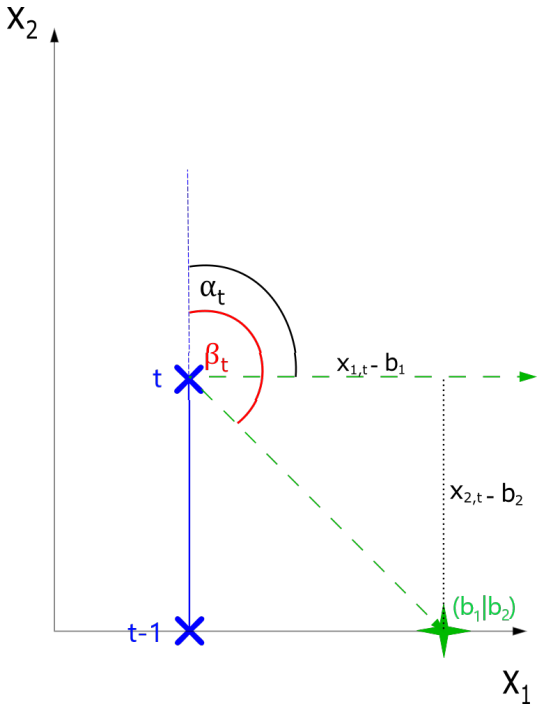

Figure 3.4: Simulation of the bearing measurement by the agent. The bearing to the landmark β_t differs from the bearing to the compass direction α_t. The closer the landmark is to the agent, the greater the difference between β_t and α_t. Crosses show positions of the agent, blue dashed lines show the direction of heading. Measured variables in red. Compass and landmark direction in green. Landmark position at $(b_1|b_2)$ marked as green star.

In this model, it is assumed that the agent wrongly believes that each landmark is at infinite distance. The agent therefore uses the landmark as a compass. In figure 3.4 it is shown, that the bearing β_t to the landmark, however, deviates from the bearing α_t to the assumed compass bearing. This deviation is greater the closer the landmark is to the agent.

β_t can be calculated as the sum of two angles. One of them is equal to the angle α_t. The other angle can be calculated using the arc tangent, since the Cartesian coordinates of the agent $(x_{1,t}|x_{2,t})$ and those of the landmark $(b_1|b_2)$ are known. The measurement of the agent $\hat{\beta}_t$ is then obtained by adding errors to β_t.

$$\beta_t = \alpha_t + arctan2((x_{2,t} - b_2), (x_{1,t} - b_1)) \tag{3.10}$$

$$\hat{\beta}_t = \beta_t * \epsilon_{*,t} + \epsilon_{+,t} \tag{3.11}$$

The x_1-axis is set so that the position of the landmark is on the x_1-axis. Thus, at the starting point $t = 0$, the agent has a bearing to the landmark of $\beta_0 = 0$. Even after leaving the starting point, the agent assumes that the landmark is still in the x_1-axis direction from its perspective. The measured $\hat{\beta}_t$ then corresponds to the estimated heading, just like $\hat{\alpha}_t$ does in the model of real compass usage.

$$\hat{\eta}_t = \hat{\beta}_t \tag{3.12}$$

As a result, a wrong heading and thus a wrong new position is estimated. This misjudgement of the agent's position is illustrated in figure 3.5.

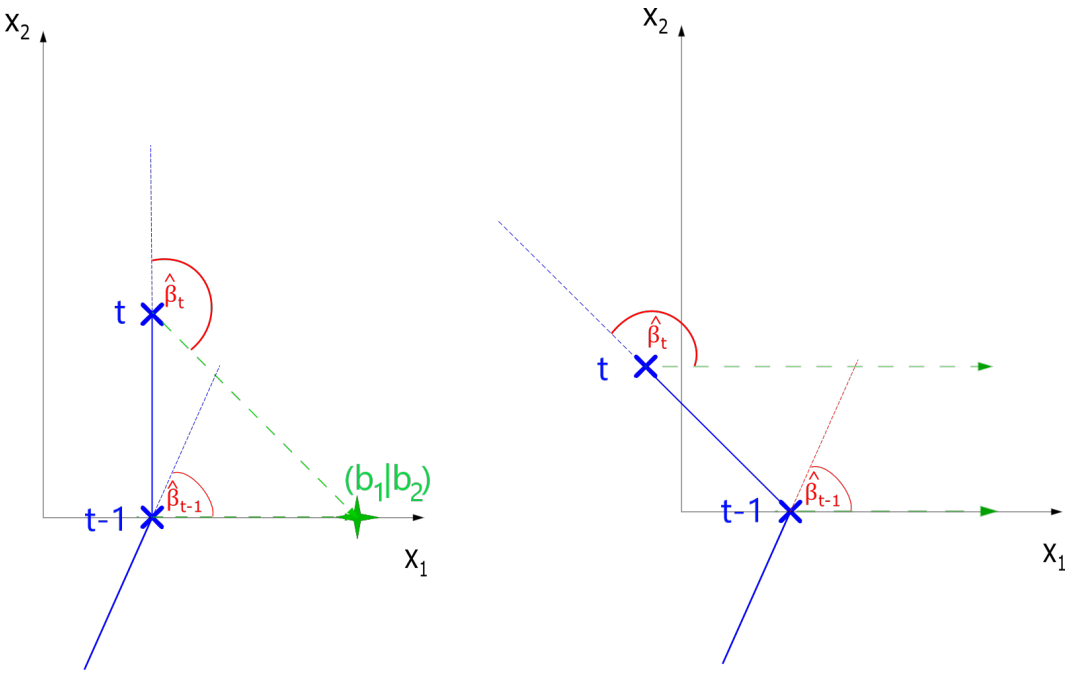

Figure 3.5: Left: The bearings relative to landmarks at a finite distance are measured by the agent. The actual, fixed path on which the agent is walking is shown. **Right**: In this figure, the erroneous, estimated path of the agent can be seen. Since the agent assumes that the bearings were measured relative to the compass direction, it estimates its own heading change to be greater than it actually is. The resulting position estimate therefore deviates from the actual position. Crosses show positions of the agent, blue dashed lines show the direction of heading. Measured variables in red. Compass and landmark direction in green. Landmark position at $(b_1|b_2)$ marked as green star.

3.2.3 Optic Flow (LM_OF)

Optic flow describes the shift of image points in the visual field when the agent moves. Through this perception, direct conclusions can be drawn about one's own movement.
The perceived bearing of a landmark in the agent's visual field changes during movement. As in the previous model, due to missing distance information, it is assumed that the landmark is at an infinite distance. Therefore, this bearing change is directly interpreted as a rotation, i.e. as a change in heading. The agent obtains the current heading by integrating the bearing changes at each step. As with odometry, it is to be expected that this integration also leads to an accumulation of errors.

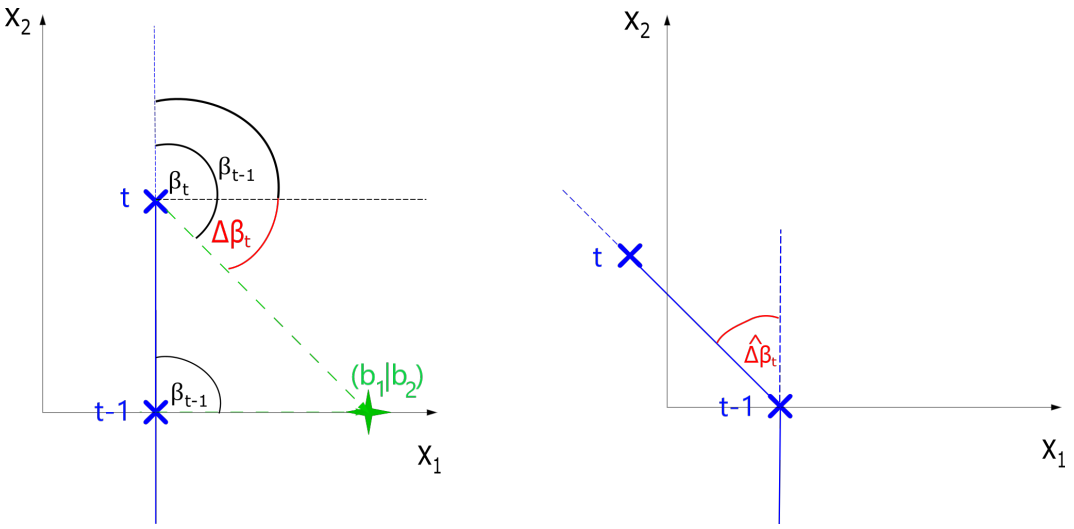

Figure 3.6: Left: The actual, fixed path on which the agent is walking is shown. $\Delta\beta_t$ corresponds to the change in bearing, i.e. the change in landmark direction in the visual field that the agent perceives. The bearings themselves are unknown to the agent, it only measures the change in bearing during a step. **Right**: Resulting erroneous position estimate by the agent. Since the agent uses the landmark as a compass, the change in bearing $\hat{\Delta\beta}_t$, i.e. the displacement of the landmark in the visual field, corresponds directly to the change in heading. This erroneous assumption leads to an estimated position deviating from the true one. Crosses show positions of the agent, blue dashed lines show the direction of heading. Measured variables in red. Compass and landmark direction in green. Landmark position at $(b_1|b_2)$ marked as green star.

With this type of path integration, the existing landmark is again assumed to be infinitely far away. Compared to LM_COMP, however, it is not the bearing

itself that is measured here, but the change in bearing $\Delta\beta_t$, as can be seen on the left in figure 3.6.

$$\Delta\beta_t = \beta_t - \beta_{t-1} \tag{3.13}$$

$$\hat{\Delta\beta}_t = \Delta\beta_t * \epsilon_{*,t} + \epsilon_{+,t} \tag{3.14}$$

The changes in bearing $\hat{\Delta\beta}_t$ are interpreted as a change in the agent's own orientation (see figure 3.6 right). Therefore, the sum of all bearing changes gives the current heading with a start heading of $\eta_0 = 0$ (in x_1-axis direction).

$$\hat{\eta}_t = \hat{\eta}_{t-1} + \hat{\Delta\beta}_t \tag{3.15}$$

As with the model of ODO, the error contained in $\hat{\Delta\beta}_t$ accumulates.

3.3 Idiothetic and Allothetic Path Integration

3.3.1 Knowledge of Landmark Position (LM_POS)

In this model, the combination of idio- and allothetic information is used to compensate for the respective errors and problems. On the one hand, the problem of error accumulation does not occur. Since the agent measures the bearing, the current heading can be determined directly. It does not have to be determined by integrating the rotational steps as in the models of ODO and LM_OF. On the other hand, the error is avoided which arises when landmarks are wrongly assumed to be infinitely far away. In this model, the landmark is not assumed to be infinitely far away. For this, the agent must determine the position of the landmark during the first steps. This is possible when the own position is determined with the help of odometry. Using the bearing to the landmark at two different positions, the landmark position can then be calculated based on the agent's own positions. Once the position of the landmark is known, bearing measurements can provide correct information about the current heading.

3.3.1.1 Determination of Landmark Position using Odometry and Bearing

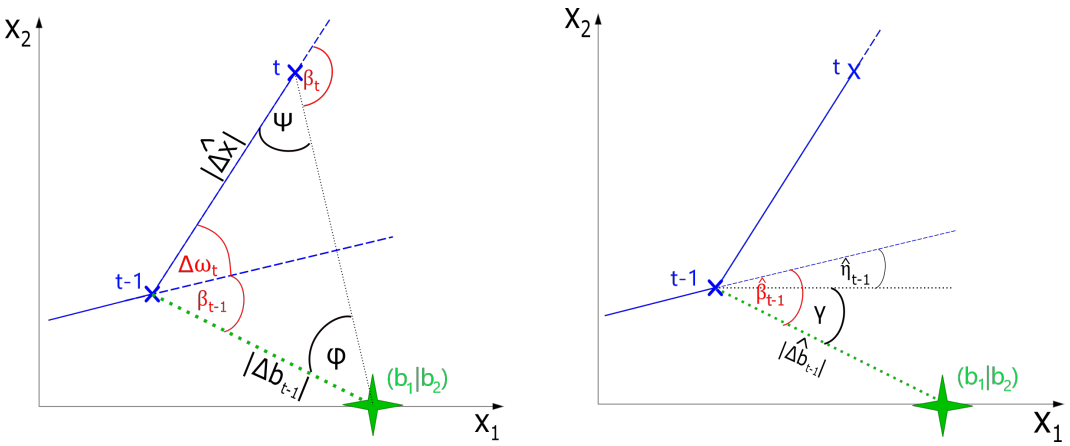

Figure 3.7: Left: The agent measures the bearings β_t and β_{t-1} and the heading change $\Delta\omega_t$. Using these measurements, the landmark distance $|\Delta\hat{b}_{t-1}|$ can be calculated. The own position is determined by $\Delta\omega_t$ as in ODO. **Right**: With the previous heading $\hat{\eta}_{t-1}$ and calculated landmark distance $|\Delta\hat{b}_{t-1}|$, the landmark position can then be calculated starting from the agent's own previous position $(x_{1,t-1}|x_{2,t-1})$. Crosses show positions of the agent, blue dashed lines show the direction of heading. Measured variables in red. Compass and landmark direction in green. Landmark position at $(b_1|b_2)$ marked as green star.

The following procedure for calculating the landmark position is shown in figure 3.7. This happens at the beginning of the path, during the first steps of the agent. Using the bearings β_t and β_{t-1} and the heading change $\Delta\omega_t$, the distance of the landmark to the agent's position $|\Delta b_{t-1}|$ at time $t-1$ can be calculated. For this, the angular quantities of the auxiliary angles ψ and ϕ need to be calculated first.

$$\hat{\psi} = \pi - \hat{\beta}_t \tag{3.16}$$

As the sum of the angles in a triangle equals to 180 degrees, $\hat{\phi}$ can be obtained:

$$\hat{\phi} = \pi - ((\hat{\beta}_{t-1} + \hat{\Delta\omega}_t) + \hat{\psi}) \tag{3.17}$$

Now the interior angles of the left triangle in figure 3.7 are known. Since the step size $|\Delta x|$ is fixed and known to the agent, the distance to the landmark $|\Delta b_{t-1}|$ can now be calculated using the law of sines. The law of sines states:

$$\frac{|\Delta\hat{b}_{t-1}|}{sin(\hat{\psi})} = \frac{|\hat{\Delta x}|}{sin(\hat{\phi})} \tag{3.18}$$

From this the distance to the landmark at time $t-1$ follows:

$$|\Delta\hat{b}_{t-1}| = \frac{|\hat{\Delta x}| * sin(\hat{\psi})}{sin(\hat{\phi})} \tag{3.19}$$

At any time, the agent has an estimate of its own heading $\hat{\eta}_{t-1}$ from the previous step and can measure the bearing $\hat{\beta}_{t-1}$. The auxiliary angle γ is then calculated as:

$$\hat{\gamma} = \hat{\beta}_{t-1} - \hat{\eta}_{t-1} \tag{3.20}$$

Using γ, the landmark position $(b_1|b_2)$ can now be estimated relative to the agent's position at time $t-1$ with:

$$\hat{b}_1 = \hat{x}_{1,t-1} + cos(\hat{\gamma}) * |\Delta\hat{b}_{t-1}| \tag{3.21}$$

$$\hat{b}_2 = \hat{x}_{2,t-1} + sin(\hat{\gamma}) * |\Delta\hat{b}_{t-1}| \tag{3.22}$$

The values $\hat{\beta}_t$, $\hat{\beta}_{t-1}$ and $\hat{\Delta\omega}_t$, which are used to calculate the landmark position, are not exact but include an additive and multiplicative error. Therefore, the estimation of the landmark position is not exact either. The estimate can be improved if the landmark position is estimated again in further steps and then all estimates are averaged to narrow down the exact landmark position.

3.3.1.2 Determination of Agent's Position using Bearing and Landmark Position

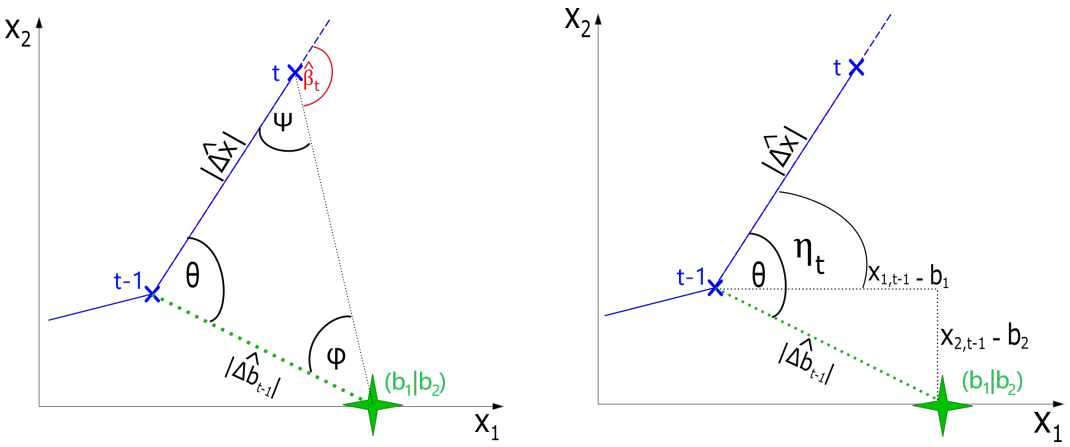

Figure 3.8: Left: The true trajectory of the agent can be seen. The agent measures the current bearing and can determine θ with known values. **Right**: With θ and known landmark position, the required heading $\hat{\eta}_t$ can then be calculated, with which the own position is estimated. Crosses show positions of the agent, blue dashed lines show the direction of heading. Measured variables in red. Landmark direction in green. Landmark position at $(b_1|b_2)$ marked as green star.

Once the landmark position is known, the agent can use it to determine its heading at each step. In order to do this, θ must be determined first. For this ψ and ϕ are needed. The respective quantities are shown in figure 3.8. $\hat{\psi}$ is calculated the same way as in the last section:

$$\hat{\psi} = \pi - \hat{\beta}_t \tag{3.23}$$

$|\Delta\hat{b}_{t-1}|$ is obtained with the Phytagorean theorem:

$$|\Delta\hat{b}_{t-1}| = \sqrt{(\hat{x}_{1,t-1} - \hat{b}_1)^2 + (\hat{x}_{2,t-1} - \hat{b}_2)^2} \tag{3.24}$$

Using the law of sines from equation 3.18, $\hat{\phi}$ can be calculated:

$$\hat{\phi} = asin\left(\frac{|\hat{\Delta x}| * sin(\hat{\psi})}{|\Delta\hat{b}_{t-1}|}\right) \tag{3.25}$$

As the sum of the angles in a triangle equals to 180 degrees, $\hat{\theta}$ can be obtained:

$$\hat{\theta} = \pi - (\hat{\phi} + \hat{\psi}) \tag{3.26}$$

As seen in figure 3.8, the current heading $\hat{\eta}_t$ can be calculated from the difference of $\hat{\theta}$ and an arc tangent:

$$\hat{\eta}_t = \hat{\theta} - arctan2(\hat{x}_{2,i-1} - \hat{b}_2, \hat{x}_{1,i-1} - \hat{b}_1) \tag{3.27}$$

By determining $\hat{\eta}_t$ independently of $\hat{\eta_{t-n}}$ from other time steps, error accumulation is avoided here. The quality of the heading estimate depends especially on the landmark position estimate. If the position of the landmark is estimated incorrectly, this will lead to a miscalculation of the heading. This miscalculation of the heading happens the same way as it does in the model of LM_COMP and the model of LM_OF, as in all cases an erroneous estimation of landmark distance is used.

4 Analysis of Results

In this chapter, the performance of the different path integration methods ODO, LM_COMP, LM_OF and LM_POS is compared under the influence of errors. COMP is not included in the comparison because this method is hardly influenced by errors and infinitely distant landmarks or compass directions are not always available in reality.

For the comparison, a fixed trajectory is specified on which the agent moves. The agent then calculates its estimated trajectory for this movement. As seen in figure 4.1, a circular path with radius 1 and slight jitter and a Lissajous curve (called "loop" in the following) are used as fixed paths. These paths are chosen as they vary in curvature. With this, specifics in the estimations that are due to the curvature characteristics of the path can be distinguished from general effects. Starting and final points are both at the origin. The circular path runs counterclockwise. The loop path starts from the origin in the first quadrant and ends in the origin coming from the third quadrant.
The fixed true trajectory, which is shown in black in the figures, is then compared with the agent-estimated trajectories shown in colour. For the comparison, the difference between the estimated final position and the true final position is measured. By limiting the comparison to the final positions, information about deviations of the estimates during the course of the path is disregarded. However, it can happen that the estimated path differs greatly from the true path and still approaches the correct final position towards the end. In the way of comparison used here, the estimate would be considered relatively correct, although the overall correctness of the path would not be very high.

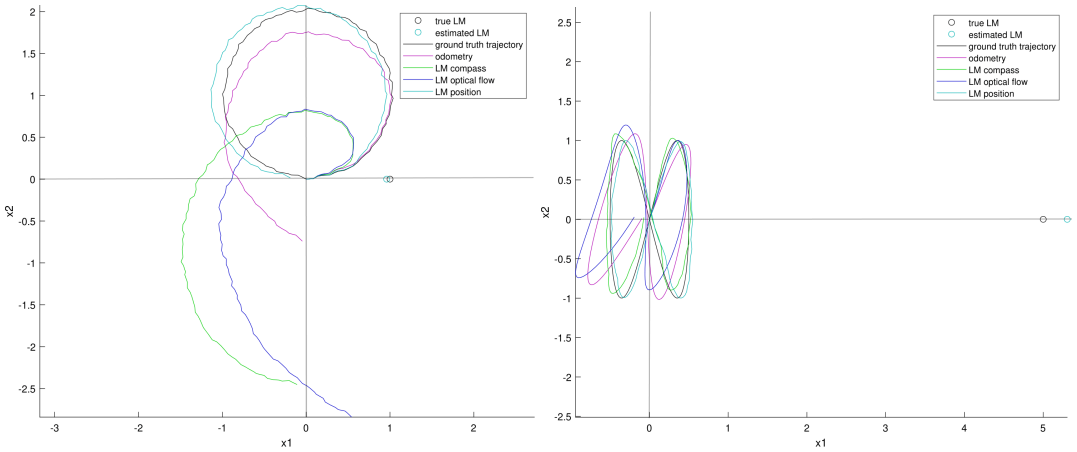

Figure 4.1: The true, fixed trajectory is shown in black as well as the estimated trajectories in different colours. The following parameters were used: Trajectory: circle, additive error: 0.1, multiplicative error: 0, landmark distance: 1 (left)/5 (right)

Different landmark distances and different additive and multiplicative error sizes are tested. The additive error size of 0.1 means, for example, that an equally distributed random absolute error out of [-0.1,0.1] is added to the measurement. The multiplicative error size of 0.1 means that the measurement is multiplied by a random value out of [0.9,1.1]. Thus a maximum relative deviation of 10% can occur.

Besides the path selection and error sizes, the landmark distance parameter affects the agent's path estimates. On the left-hand side of figure 4.1 a landmark distance of 1 can be seen, on the right-hand side the landmark is at a distance of 5 from the origin.

4.1 Distance from Estimated to True Final Position

To compare the robustness of the path integration types, the distance from the estimated final point to the true final point, which equals the starting point, is measured. If the estimation is correct, this distance is zero. In figure 4.2 to figure 4.4 below, this distance is shown depending on the landmark distance and for different parameter values for path selection and error sizes. The result values were averaged over 100 runs, vertical bars show the standard deviation of the mean values. Further figures with other parameter values can be found in chapter 6.

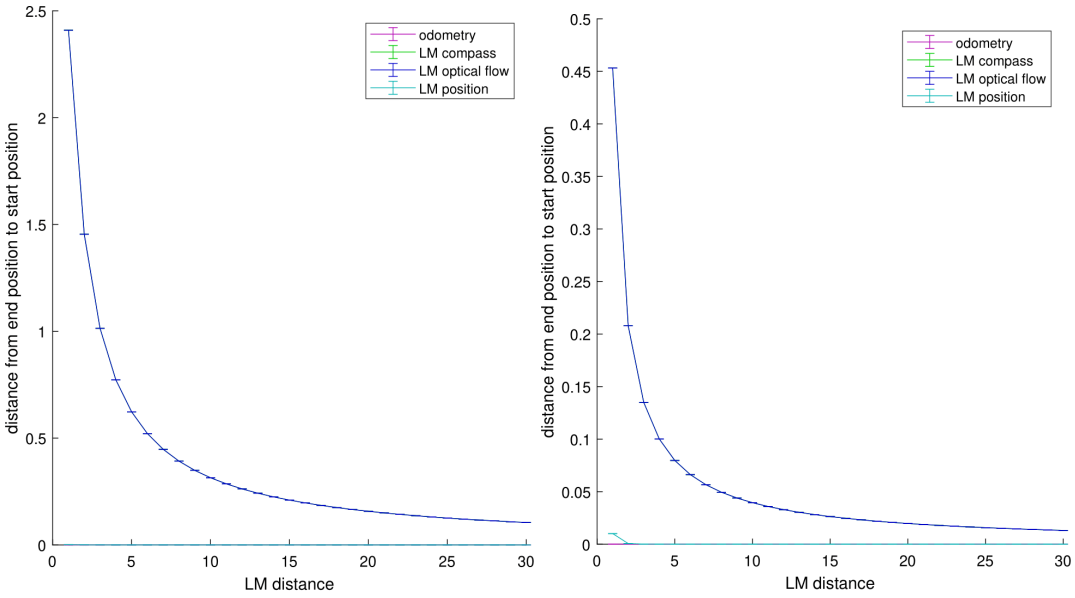

Figure 4.2: The distance error relative to the landmark position is shown with the following parameters: Trajectory: circle (left)/loop (right), additive error: 0, multiplicative error: 0 (curves for ODO and LM_POS and curves for LM_COMP and LM_OF overlap each other)

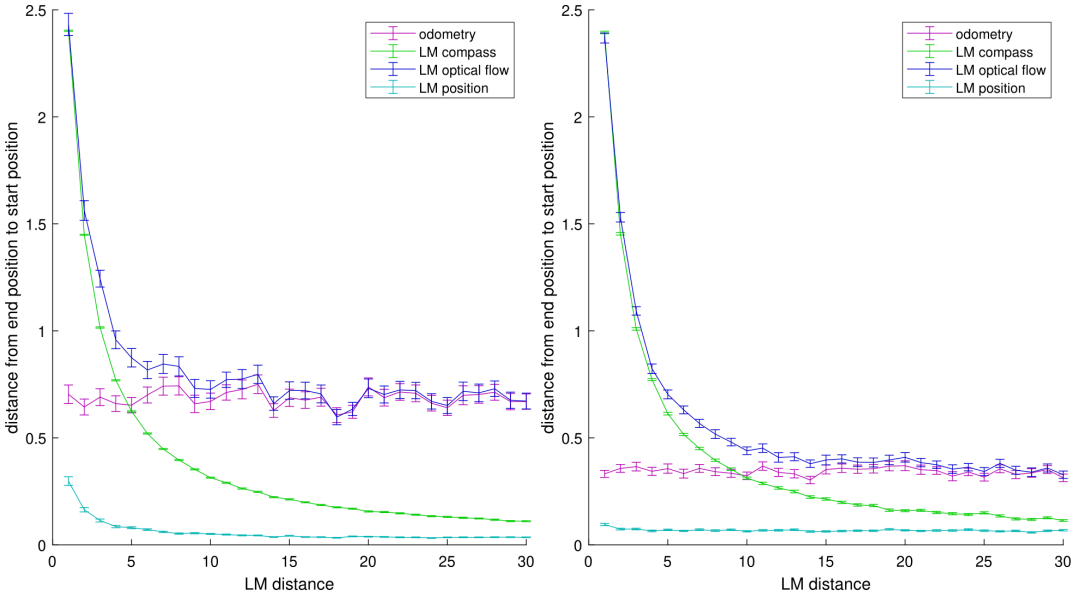

Figure 4.3: The distance error relative to the landmark position is shown with the following parameters: Trajectory: circle, additive error: 0.1 (left)/0 (right), multiplicative error: 0 (left)/0.1 (right)

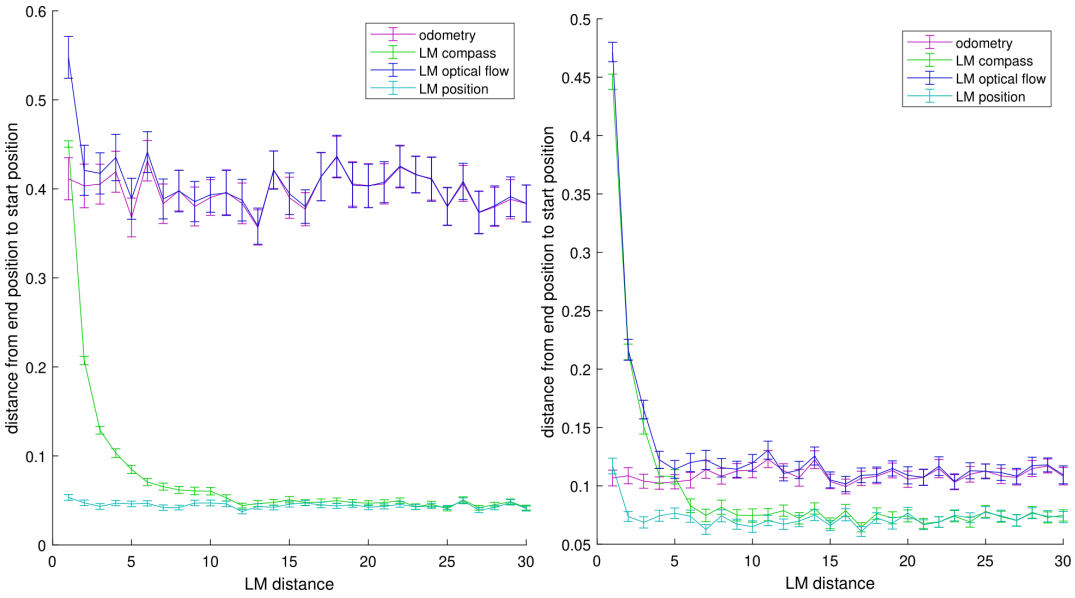

Figure 4.4: The distance error relative to the landmark position is shown with the following parameters: Trajectory: loop, additive error: 0.1 (left)/0 (right), multiplicative error: 0 (left)/0.1 (right)

4.1.1 Odometry (ODO)

Without any error, the path integration through odometry works perfectly (see figure 4.2). However, since errors are accumulated in this type of path integration, it is not very error robust once errors are added. The distance of the final position to the origin is slightly larger with the circular path (figure 4.3) than with the loop path (figure 4.4). Responsible for this are the curvature properties of the respective paths. Both the circular path and the loop path results show that an additive error of 0.1 has a greater impact than a multiplicative error of 0.1. This is because the size of the rotation steps is very small (about 0.063 rad per step for the circle path). An additive error of 0.1 therefore is greater than a multiplicative error of 0.1. The standard deviation of the mean values is also greater for an additive error of 0.1 than for a multiplicative error of 0.1.

4.1.2 Landmark Usage as Compass (LM_COMP)

Without adding an error, the quality of the estimate depends only on the distance of the landmark (see figure 4.2). The further away the landmark is, the better the estimate. For the loop, this error is generally smaller than for the circular path, even when errors are added. This is because the curvature in the loop changes during the path. Misestimates can be compensated later

on the path when the opposite curvature occurs. For additive compared to multiplicative error (compare figure 4.3 and figure 4.4 left vs. right), the estimation accuracy hardly differs. Since the error is not accumulated, the procedure is very robust. The standard deviations of the mean are thus always very small. Therefore, the accuracy mainly depends on the landmark distance.

4.1.3 Optic Flow (LM_OF)

In an error-free simulation (see figure 4.2), this type of path integration behaves exactly like LM_COMP. The accuracy of the estimate depends solely on the landmark distance.
This changes when adding an error (see figure 4.3 and figure 4.4). In this model, as in ODO, the errors accumulate and can no longer be compensated for later. Therefore, this method shows two weaknesses at the same time and is thus the least error-robust. The first weakness is the following: If the landmark is very close, the error due to the wrong assumption of the infinitely distant landmark is more significant. Due to this, for close landmarks, the graph of LM_OF is very similar to the graph of LM_COMP. The other weakness ist that the further away the landmark, the larger the relative impact of the accumulated error. Therefore, for more distant landmarks, the graph of LM_OF resembles the graph of ODO.

4.1.4 Knowledge of Landmark Position (LM_POS)

In this model, accurate estimates are achieved when there is no error influencing the estimates (see figure 4.2). However, once multiplicative or additive errors are added (figure 4.3 and figure 4.4), errors in landmark position estimation occur during the first steps. That leads to an error during the rest of the path estimation.
This type of path integration does not accumulate errors and also depends very little on the distance of the landmark. For close landmarks, there is sometimes a slightly larger error, as misestimates of the landmark position have a larger effect on the path estimation than for very distant landmarks. For example, if the landmark position is misestimated by one unit, this will make a bigger difference at a landmark distance of 1 to the origin than at a distance of 30 or greater. This is because the angular deviation of measured bearing and theoretical bearing to a landmark at the estimated position depends on the landmark distance. For close landmarks this angular deviation is larger than for distant landmarks even if the distance between true and estimated landmark position is the same. Overall, however, the estimation is very accurate with both additive error and multiplicative error and only shows small standard deviations of the mean values. It shows the best results compared to the other methods.

4.2 Final Positions: Statistical or Systematic Errors

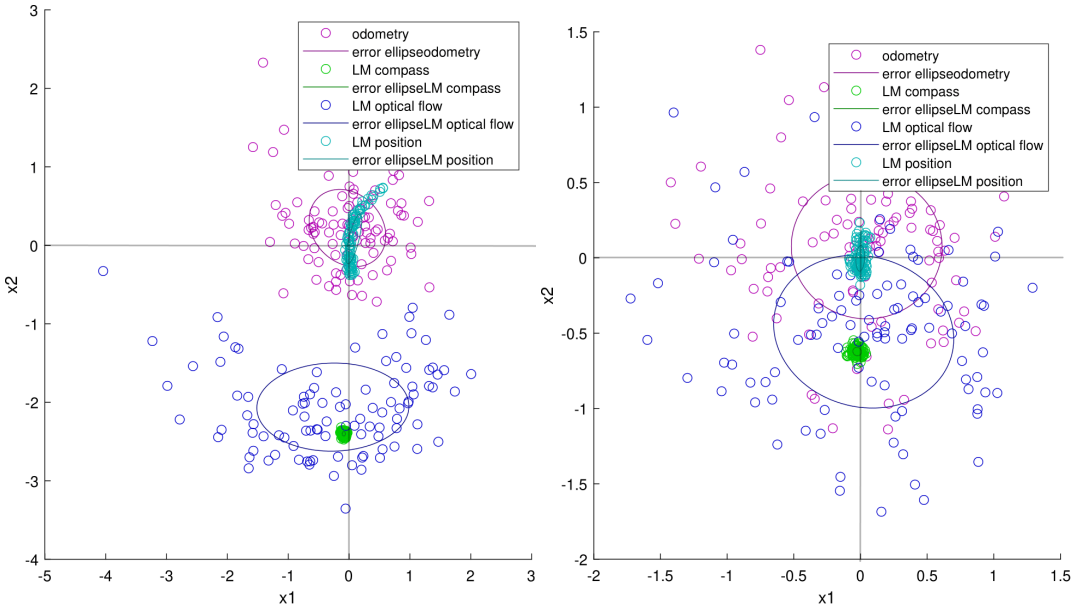

Figure 4.5: The final position error is shown with the following parameters: Trajectory: circle, additive error: 0.1, multiplicative error: 0, landmark distance: 1 (left), 5 (right)

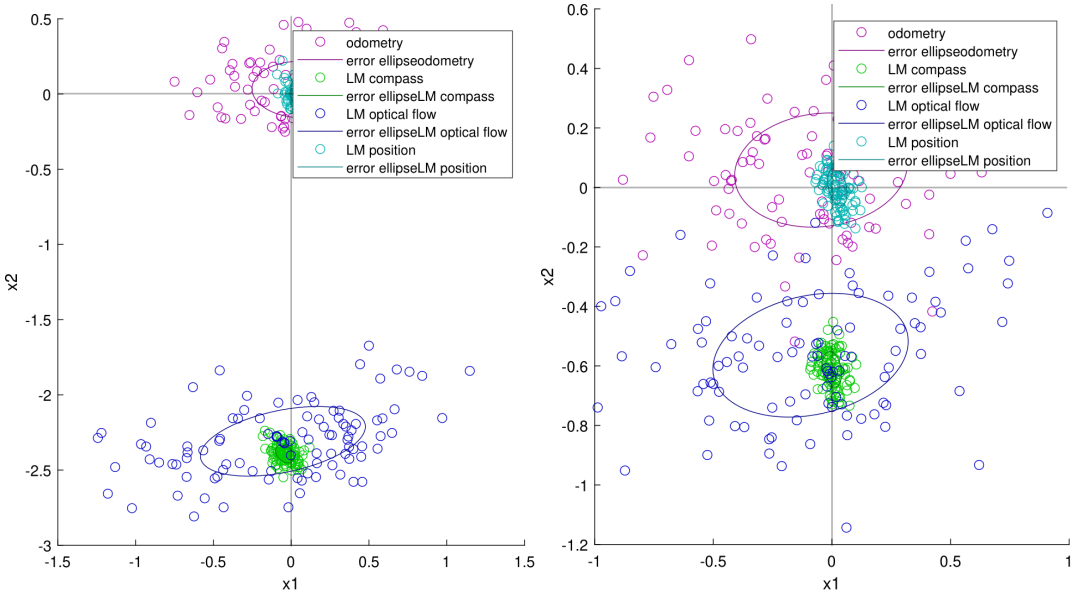

Figure 4.6: The final position error is shown with the following parameters: Trajectory: circle, additive error: 0, multiplicative error: 0.1, landmark distance: 1 (left), 5 (right)

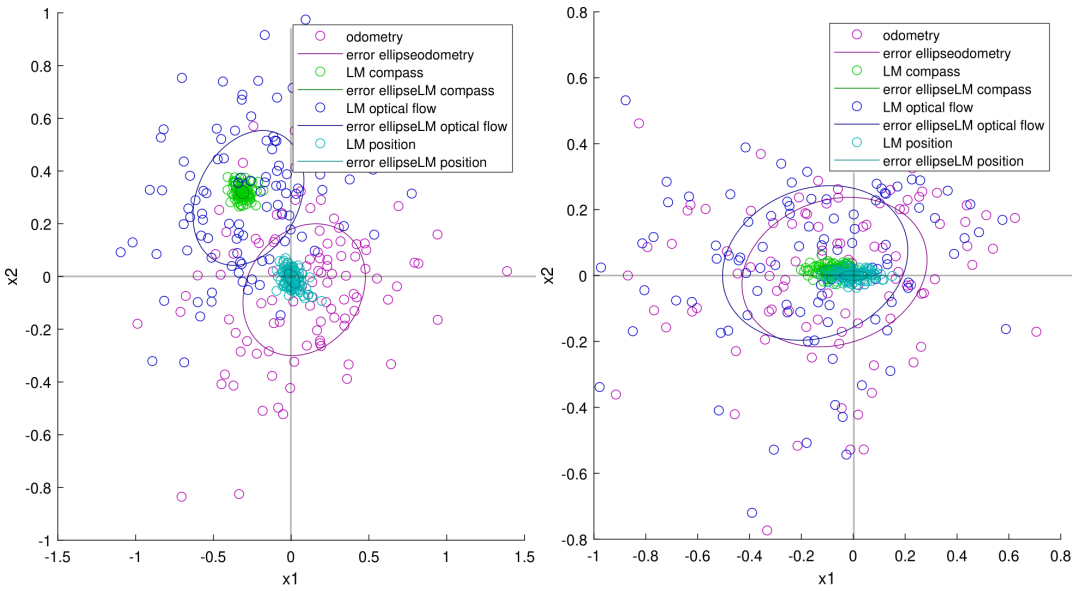

Figure 4.7: The final position error is shown with the following parameters: Trajectory: loop, additive error: 0.1, multiplicative error: 0, landmark distance: 1 (left), 5 (right)

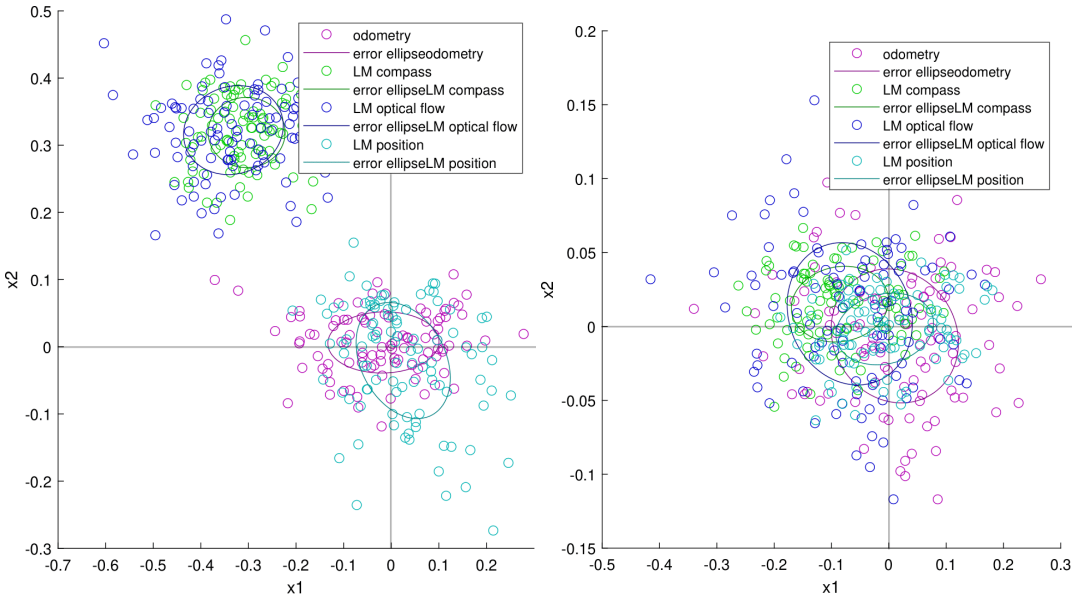

Figure 4.8: The final position error is shown with the following parameters: Trajectory: loop, additive error: 0, multiplicative error: 0.1, landmark distance: 1 (left), 5 (right)

In figure 4.5 to figure 4.8 the estimated final positions are shown, i.e. the positions where the agent believes to be after the path has been completed.

The true final position is always at the origin at (0|0). For each type of path integration, 100 final positions are estimated depending on error sizes, path selection and landmark distance. The size of the error ellipses shows the statistical error, i.e. the scattering of the values. The systematic error is the mean deviation of the values from the origin in a certain direction. It is represented by the centre of the error ellipses compared to the origin. Further figures with other parameter values can be found in chapter 6. There, examples for the estimated trajectories are shown on the left sides of the error ellipse figures to show how the complete courses of the estimated trajectories look like.

4.2.1 Odometry (ODO)

Since the final positions are equally distributed in all directions around the origin, this is mainly a statistical error, while hardly any systematic error can be seen.
However, it can be observed that the final position varies more in x_1-direction than in x_2-direction (see e.g. figure 4.6). This is because of the chosen paths and their curvature properties. The error is more pronounced with an additive error than with a multiplicative error. In this case, the scatter is more than twice as large (compare figure 4.5 and figure 4.6). In addition, the statistical error is greater for the circular path than for the loop path (compare, for example, figure 4.6 and figure 4.8), which is due to the curvature properties of the paths. Since both right and left curvatures occur in the loop, errors can be partially compensated for in the course of the path. This is not the case with the circular path, where there is only a left-hand curvature.
Here, the estimate does not depend on the landmark position.

4.2.2 Landmark Usage as Compass (LM_COMP)

A strong systematic error can be seen here, while the statistical error is very small. The systematic error becomes smaller with increasing landmark distance. In general, the estimated final positions for the circular path are at around $x_1 = 0$ with a negative x_2-value (see e.g. figure 4.5). This is because the landmark is assumed to be a compass. It causes the rotation step sizes to be overestimated in the first half of the circular path and underestimated in the second half. As a result, the agent first estimates a stronger curvature and later a weaker one. This leads to an estimated path of a spiral whose final point is in the negative x_2-range. The described shape can be seen in figure 4.1 on the left-hand side. The effect is not as strong with the loop path, as the curvatures vary more at each step and therefore the effect is partially compensated for.
The systematic error in the loop path is very small even for close landmarks,

as can be seen in figure 4.7. Here the estimated final position is on average in the slightly positive x_2- and slightly negative x_1-range.
Since LM_COMP is very robust against both multiplicative and additive errors, the different errors hardly show any difference in the final position estimate (compare e.g. figure 4.5 and figure 4.6).

4.2.3 Optic Flow (LM_OF)

Since LM_OF combines the errors of ODO and LM_COMP, this type of path integration shows both a systematic and a statistical error (see e.g. figure 4.5). These are both stronger for the circular path than for the loop path (compare e.g. figure 4.5 and figure 4.7). This is, as described in subsection 4.2.1 and subsection 4.2.2, due to the curvature properties of the chosen paths. Similar to LM_COMP, in LM_OF the systematic error decreases with increasing landmark distance. (see figure 4.5). As also seen in ODO, LM_OF is more sensitive to the additive error than the multiplicative error, hence the statistical error is larger with additive error (compare e.g. figure 4.5 and figure 4.6).

4.2.4 Knowledge of Landmark Position (LM_POS)

With this type of path integration, independent of the parameter values, there is hardly any systematic error and only a very small statistical error (see figure 4.5 to figure 4.8). It is noticeable that the final positions for the circular path with close landmark and additive error (figure 4.5) deviate very strongly in x_2-direction. This is due to the misestimation of the landmark position. The landmark position estimation is more prone to the additive error. Therefore, an additive error amplifies the effects as described below:
If the landmark is estimated too far away, the estimated final position for the circular path tends to be in the negative x_2-range. This is because, as with LM_COMP, the curvature is overestimated during the first half of the path and underestimated during the second half. This results in a spiral path similar to LM_COMP. If the landmark is estimated too close, it has the opposite effect. The resulting spiral path has a weak curvature at first, which becomes increasingly stronger.
The misestimation of the landmark position also has a greater effect on the estimated angles if the landmark is estimated too close. The error of angle estimation is larger if a landmark located at position (10|0), for example, is estimated at (1|0) than if it is estimated at (19|0) (see figure 4.9).

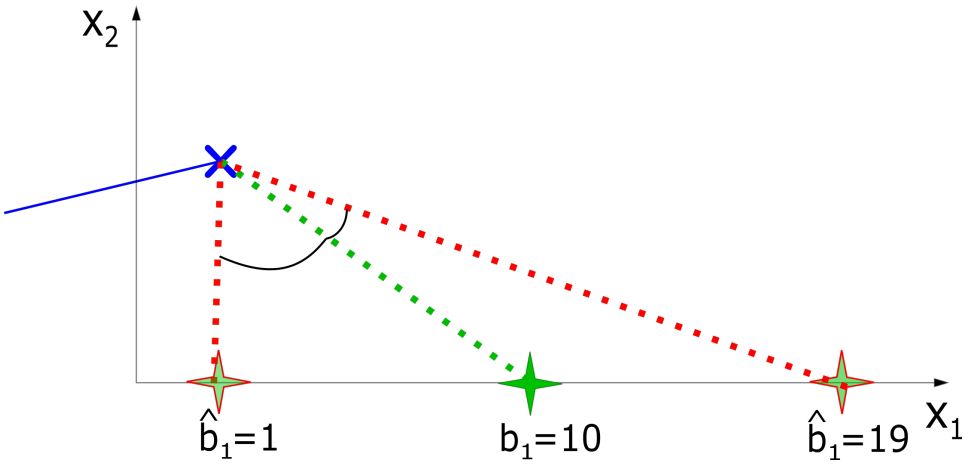

Figure 4.9: The angle from the agent between the landmark positions at (1|0) and (10|0) is greater than that between the landmark positions at (10|0) and (19|0). Therefore, the misestimation of the landmark position has a greater impact on the use of the measured angle when the landmark is estimated too close. Crosses show positions of the agent, landmark direction in green. Landmark position at $(b_1|b_2)$ marked as green stars. Left landmark estimate is too close, right landmark estimate is too far away.

Therefore, the deviation of the final positions seen in the circular path with close landmark and additive error in figure 4.5 is stronger in positive x_2-direction than in negative x_2-direction. For the same reason, this error becomes less relevant with increasing landmark distance.
Since the curvatures vary for the loop path, the effect is not as pronounced for this path (see figure 4.7).

4.3 Overall Analysis

LM_OF contains larger statistical and systematic errors and therefore shows the worst error robustness. This is because both the accumulation of error and the misestimation of landmark distance worsen the estimate here. The accumulation of error directly affects the statistical error. The misestimation of the landmark distance leads to a systematic error. It should be noted here that the poor performance relates to the highly simplified model and not the general use of optic flow. In reality with optic flow, there are many more image points available in the visual field.

ODO and LM_COMP are mainly affected by only one of these two sources of error that occur in LM_OF. Which of these two types of path integration works better depends on landmark distance. Above a certain distance, a landmark

is a good enough compass to give better estimates than the path integration with ODO. From which landmark distance this applies depends on the error sizes used. This is because ODO is affected by error accumulation and shows relatively constant errors regardless of the landmark distance. In addition, it is important to note which types of errors occur. Whether LM_COMP or ODO gives better results depends on the prioritisation of good precision (small statistical error) or high accuracy (small systematic error). Since LM_COMP mainly leads to a systematic error due to the misestimation of the landmark distance and shows hardly any statistical error, this type of path integration shows high precision. The precision of LM_COMP can be very useful. This is because when the path is run repeatedly, the agent always arrives at approximately the same position. This error can be learned by the agent and thus predicted. This is not possible with ODO with large statistical error.

LM_POS does not accumulate error. Furthermore, if the distance of the landmark is estimated correctly, it does not contain the systematic error that occurs in LM_COMP. Overall, LM_POS therefore shows the best error robustness. Even though it differs only slightly from LM_COMP for very distant landmarks, LM_POS consistently shows a better estimate. It can thus be seen that the combination of idio- and allothetic information leads to better path integration than when only one type of information is considered at a time.
It should be noted, however, that LM_POS involves additional computational effort. This is particularly worthwhile for close landmarks, as LM_POS is by far the most error-resistant method in these cases. For more distant landmarks, the performance of LM_COMP is good enough, so that the additional computational effort only brings a very small improvement in the estimate.

5 Discussion and Outlook

5.1 Assessment of Results

5.1.1 Separation of the Term of Path Integration

The analysis of the path integration models shows that path integration using idiothetic and allothetic information gives the best results. This indicates that it makes sense to study idio- and allothetic path integration together. Often, studies on path integration only consider purely idiothetic path integration. The concept of idiothetic path integration is clearly separated from other spatial orientation methods that use allothetic information, such as optic flow, SLAM and spatial updating.

This work however shows how closely related, for example, conventional idiothetic path integration by odometry and the determination of self-rotation by using optic flow are. The only difference is in the way the information about the rotation step is obtained, idio- or allothetically. The remaining path calculation works identically for ODO and LM_OF. Also with the other types of path integration the calculation of the path works the same, the only difference in each case is how the heading is determined.

Depending on whether more idiothetic or allothetic information is used for this calculation, the type of path integration can be arranged on a spectrum ranging from pure idiothetic path integration to pure allothetic path integration.
Other types of localisation can then be placed on this spectrum: SLAM can be compared to LM_POS as in both cases odometric information as well as information from landmarks with unknown positions are available. This information can then be used to determine one's own position and the landmark positions. SLAM should therefore be placed in the middle of the spectrum, as both idio- and allothetic information is used.

The method of spatial updating also has great similarities with the path integration methods described here. Spatial updating describes the ability to continuously locate points in the environment that are no longer visible while moving. With this information, the position of the points in the environment is updated relative to one's own position (Wolbers et al., 2008). Since with path integration the own position is continuously calculated relative to the origin,

or with LM_POS the own position is determined starting from the landmark position, the procedures are very similar to spatial updating. The difference is mainly the reference point, which can be either the own position or a position in the environment. This only changes the way the information is represented (see subsection 5.1.4), but not the process of the method.
The two methods are even more similar if one assumes that spatial updating is used to predict expectation values for the bearing to the landmark for possible positions of the agent. These predicted values could then be compared with the perceived landmark bearing. The prediction that is closest to the actual perception is then used to deduce the agent's own position. Since expected values can not be calculated for all possible positions, an estimate could be made in advance of which positions are most likely. This prediction can be made with the help of odometry, for example.
Matching actual measurements with stored scenarios is also similar to snapshot homing. With this method, an agent can return to a known position by matching the current environment with the stored snapshot of the environment at the destination (Cartwright & Collett, 1983).

This shows, that other methods of localisation are very closely related to the concept of path integration used here, and can even be placed directly on a spectrum that ranges from idiothetic to allothetic path integration. That finding suggests that too much attention is given to the distinction and conceptual separation of the different types of orientation. It shows that a collective term represents the similarities of these concepts better.
In their study on self-localisation, Klatzky et al. already used such an collective term for idiothetic path integration and allothetic localisation (Klatzky et al., 1998). There, the term spatial updating of self-position is used synonymously with the term path integration used in this work. Both times it is about updating one's own position step by step.
It becomes evident that a joint investigation of idiothetic and allothetic orientation procedures makes sense. On the one hand because of overlaps in content and on the other hand because it could be shown in this work that this combination leads to better performance.

5.1.2 Classification of Landmarks: Global or Local

Yesiltepe et al. classify landmarks as global and local landmarks depending on their visibility. Global landmarks are visible from a large amount of positions and therefore also from a greater distance. Local landmarks are only visible in the immediate surrounding area and are therefore usually close to the agent. Global landmarks can be more helpful for agents who are unfamiliar with the environment. Whereas local landmarks can be more useful for agents who are familiar with the environment (Yesiltepe et al., 2020).

In this work, landmarks are not distinguished by visibility but by distance. However, the visibility of a landmark correlates with distance. Global landmarks are mostly landmarks that are still visible from far away. While local landmarks, i.e. landmarks that are only visible from a few places, are usually located close to the agent.

It has been shown in this work that distant landmarks provide error robust path integration even without a known position. The use of nearby landmarks, however, is only useful if their position is known. This could be related to the result of Yesiltepe et al. mentioned above. In unfamiliar environments, the agent has less knowledge about the environment. Global landmarks, can however, be used for path integration just like in LM_COMP, even if no knowledge about their position is available. The accuracy of the landmark position estimate is less important here. Reliable path integration is possible even with inaccurate position estimation. In a known environment, the agent may have more knowledge about the position of a landmark or can estimate it with a higher accuracy. This estimation accuracy is particularly important for close, local landmarks, as these can then be used for path integration as in LM_POS. The presented results for LM_COMP and LM_POS could therefore be classified as follows. For global landmarks LM_COMP can be used, for local landmarks the additional computational effort of LM_POS to determine the landmark position is worthwhile and comes with better accuracy.

5.1.3 Optic Flow

When analysing the different types of path integration, LM_OF is found to be the least error robust. This contradicts studies that find evidence that the information of the optic flow alone is sufficient for self-localisation (Warren & Hannon, 1988).
It should be noted that the LM_OF model does not adequately capture the real-world use of optic flow. In LM_OF the actual landmark position is ignored. Even if the landmark position was known, the problem of error accumulation would still remain. This could be compensated if the optic flow provides information from several landmarks. With the additional information, the error could be extracted and more correct positions could be estimated. In reality, this is the case because there are usually many more points in the visual field whose displacement provide information about the movement of the agent.

5.1.4 Information Representation

During path integration, the agent stores its own position and the heading for each step. The form in which this information is represented in the agent depends on the reference point relative to which the positions are determined.

The coordinate system can be anchored either allocentrically (for example, the starting point of the path is the origin) or egocentrically (the agent's position is the origin). Moreover, it is possible to store coordinates in Cartesian or polar form. Cheung and Vickerstaff looked into the question of which of these systems is least prone to errors. They came to the conclusion that a Cartesian allocentric representation gives the best results (Cheung & Vickerstaff, 2010). Therefore, in this work, the position and heading information was represented in Cartesian allocentric form.

It is debatable, however, whether a polar egocentric representation is more likely to be used by biological agents for some localisation methods. For the landmark position in LM_POS, for example, it seems plausible that the information is represented in polar egocentric form. This is because the position of the landmark is determined starting from one's own position. For the same reason, it also makes sense for spatial updating to represent the landmark positions in polar egocentric form. Whether this difference in information representation has a direct effect on the error robustness of the path integration types discussed here is unclear and can be further investigated.

5.2 Outlook

5.2.1 Distance Estimation of a Landmark with Width or Height

Since path integration with LM_POS provides the most reliable results, the simulation of this method could be further extended. The errors that occur in LM_POS are largely due to the fact that the estimation of the landmark position is erroneous. Therefore, future work could develop methods to make the landmark estimation more accurate.
For example, another way to estimate the landmark distance is to consider landmarks that are not only point-shaped but have a certain height or width. Then not only one bearing but several bearings to the outer edges of the landmark can be measured.

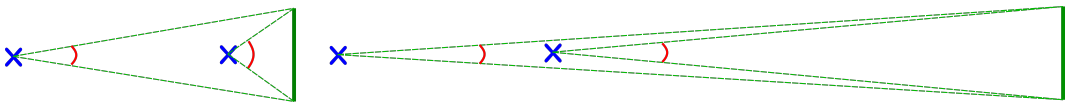

Figure 5.1: Change of the angle between the outer edges of the landmark for close (left) and distant (right) landmarks. This change can be used to infer landmark distance. Crosses show positions of the agent, blue dashed lines show the direction of heading. Measured variables in red. Landmarks in green.

When the agent walks towards a landmark, the angle between the outer edges changes more when the landmark is close to the agent (see figure 5.1). The change of the angle between the outer edges can therefore be used to infer the distance of the landmark.

5.2.2 Selection of Landmarks

In a real environment there are usually more landmarks than just one. The additional information provided by multiple landmarks can be used to compensate for measurement errors. It therefore makes sense to extend the present work to enable path integration with multiple landmarks distributed in the environment.
In order to combine the multiple measurement results, it must be decided how the respective values are weighted. One possible weighting could be the distance of the landmark. It has been shown that landmarks with a greater distance provide more reliable values. Tinbergen and Kruyt found out as early as 1938 that bee wolves select landmarks on the basis of this distance criterion (Tinbergen & Kruyt, 1938).

It is also possible that landmarks that are visible in front of the agent in direction of heading give better results than landmarks that the agent passes. This is because if the heading does not change, the bearing will remain the same when the agent walks directly towards the landmark. Small changes in heading could maybe be more accurately represented by the change in bearing, despite the unknown landmark position. The concentration on visible landmarks in the direction of the agent's heading also makes sense insofar as these are landmarks that are represented on the visual field. To get information about landmarks outside of the visual field, the agent has to turn its head or adjust the camera direction.
In addition, other criteria can be included that influence the trustworthiness of a landmark. For example, if a landmark is in motion, it may produce results that are very different from the other landmarks and should be weighted weakly or removed from the calculation.

An additional difficulty arises when using multiple landmarks. It must be possible to distinguish these landmarks from each. In order to be able to estimate the bearing change, the bearings of the same landmark must be assigned to each other. This has to be implemented in the simulation.

5.2.3 Enhanced Combination of Idio- and Allothetic Path Integration

Another possible extension of this work is to simulate types of path integration that combine idiothetic and allothetic information even more strongly. In LM_POS, idiothetic information has so far only been used to determine the landmark position. However, it is possible to combine idio- and allothetic information also during the calculation of the path. If conflicting information is provided, it must be decided which information will determine the path calculation. How the information is weighted depends on the reliability of the measurements.
The analysis of this work can be consulted in the weighting decision. For example, it has been shown that LM_COMP does not provide reliable information for close landmarks. Therefore, the weighting should be weaker in this case. The more information available, the more computational effort is needed to weigh and merge it. A stronger combination of idio- and allothetic path integration therefore leads to more complex path integration models.

6 Collection of Figures

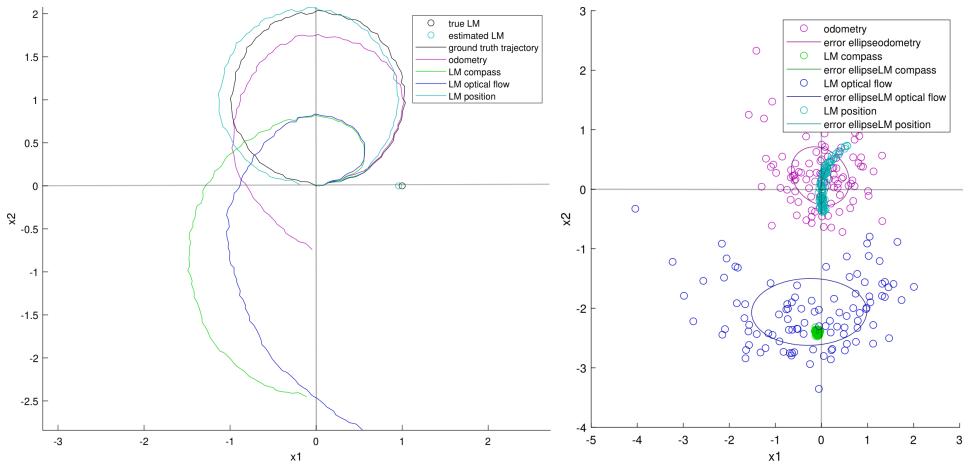

Figure 6.1: The estimated trajectories (left) are shown as well as the final position error (right) with the following parameters: Trajectory: circle, additive error: 0.1, multiplicative error: 0, landmark distance: 1

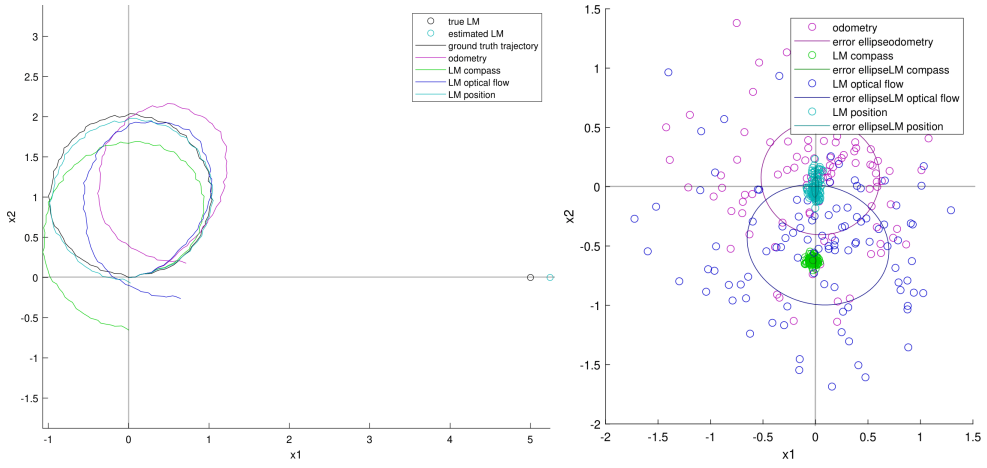

Figure 6.2: The estimated trajectories (left) are shown as well as the final position error (right) with the following parameters: Trajectory: circle, additive error: 0.1, multiplicative error: 0, landmark distance: 5

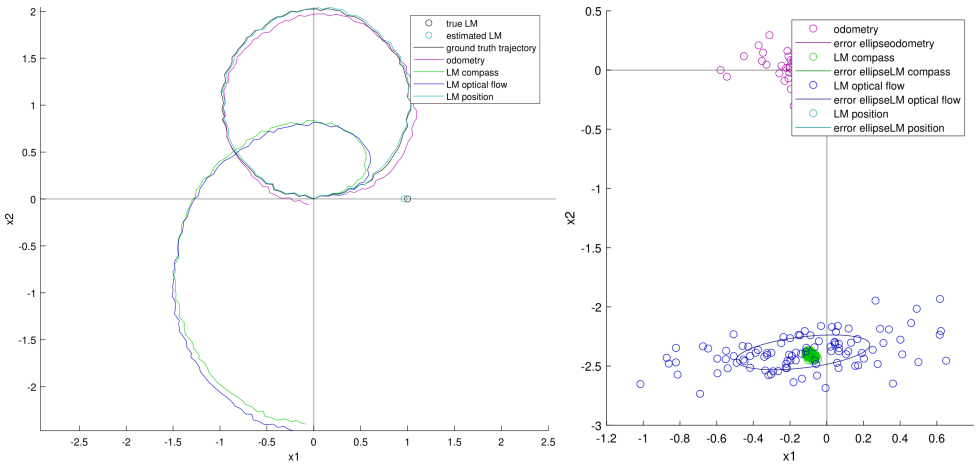

Figure 6.3: The estimated trajectories (left) are shown as well as the final position error (right) with the following parameters: Trajectory: circle, additive error: 0.025, multiplicative error: 0.025, landmark distance: 1

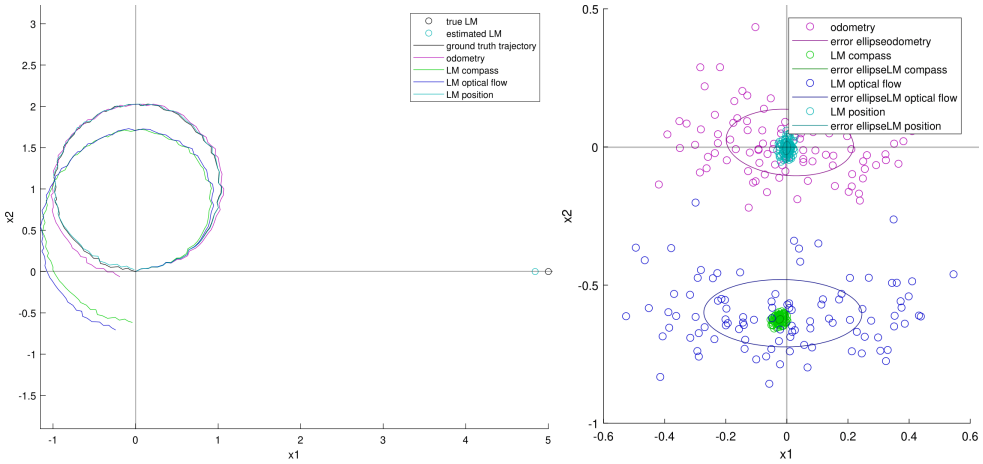

Figure 6.4: The estimated trajectories (left) are shown as well as the final position error (right) with the following parameters: Trajectory: circle, additive error: 0.025, multiplicative error: 0.025, landmark distance: 5

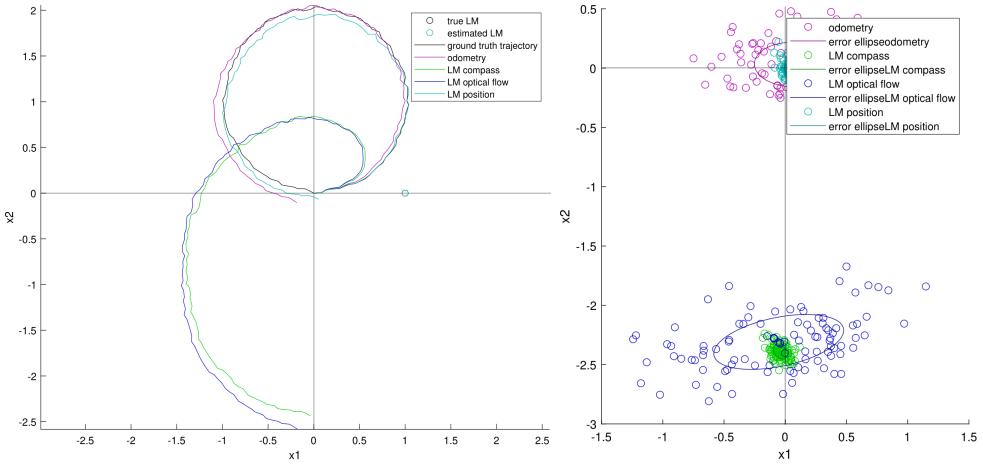

Figure 6.5: The estimated trajectories (left) are shown as well as the final position error (right) with the following parameters: Trajectory: circle, additive error: 0, multiplicative error: 0.1, landmark distance: 1

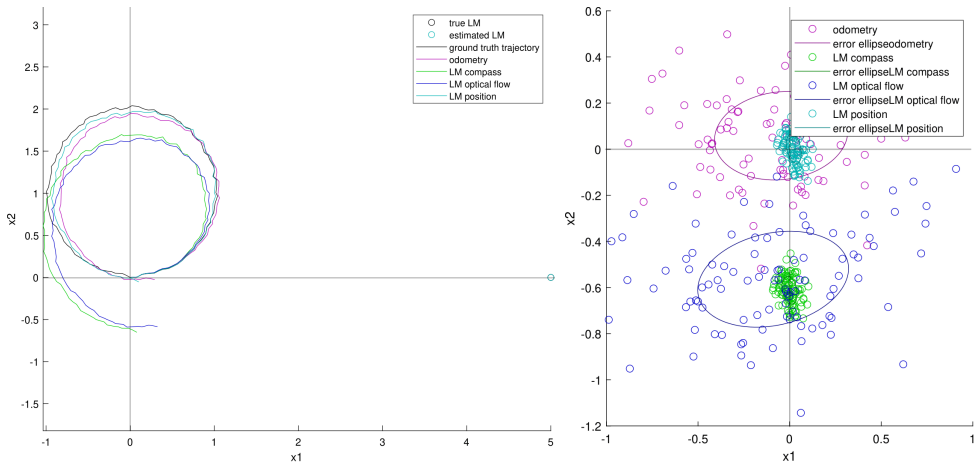

Figure 6.6: The estimated trajectories (left) are shown as well as the final position error (right) with the following parameters: Trajectory: circle, additive error: 0, multiplicative error: 0.1, landmark distance: 5

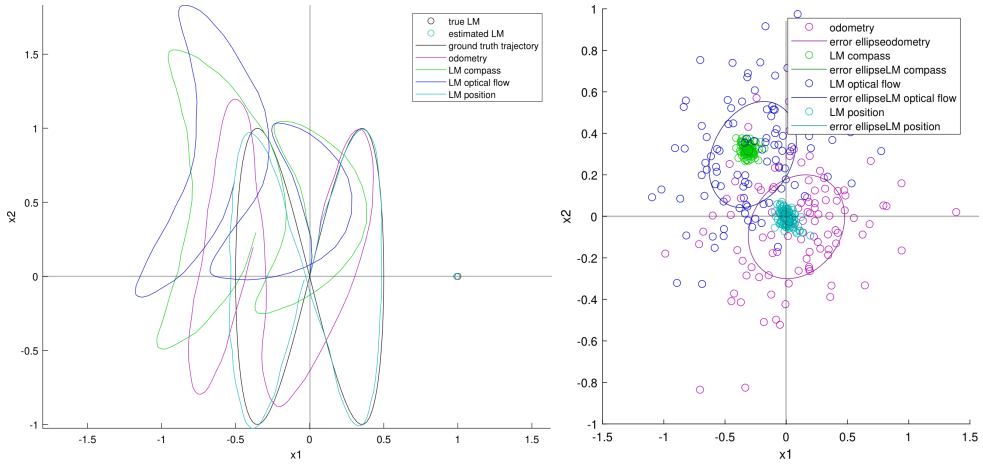

Figure 6.7: The estimated trajectories (left) are shown as well as the final position error (right) with the following parameters: Trajectory: loop, additive error: 0.1, multiplicative error: 0, landmark distance: 1

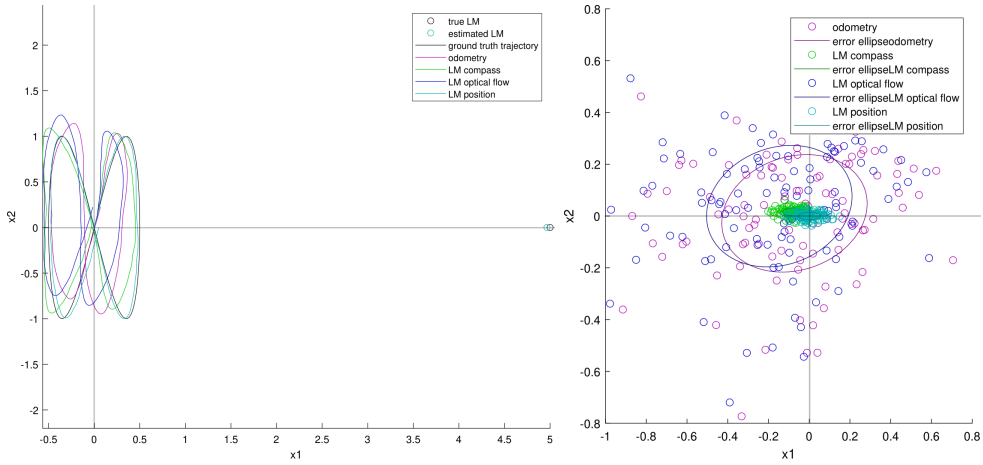

Figure 6.8: The estimated trajectories (left) are shown as well as the final position error (right) with the following parameters: Trajectory: loop, additive error: 0.1, multiplicative error: 0, landmark distance: 5

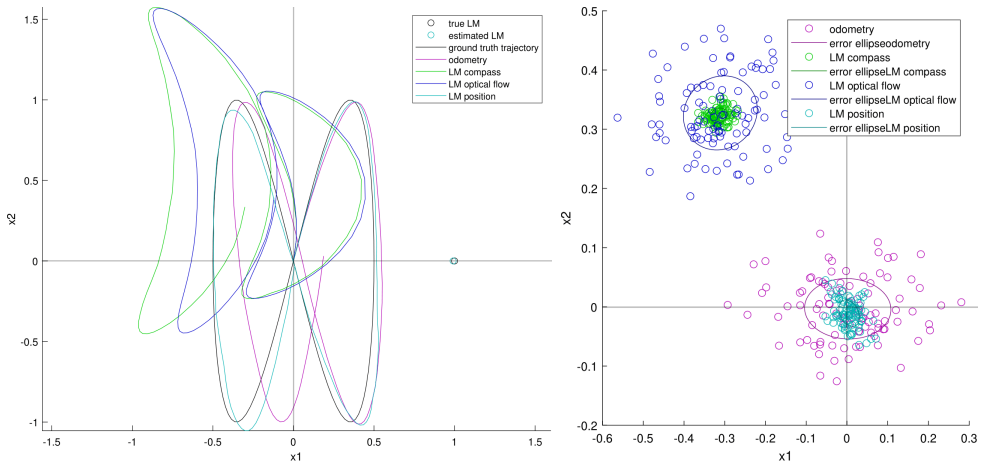

Figure 6.9: The estimated trajectories (left) are shown as well as the final position error (right) with the following parameters: Trajectory: loop, additive error: 0.025, multiplicative error: 0.025, landmark distance: 1

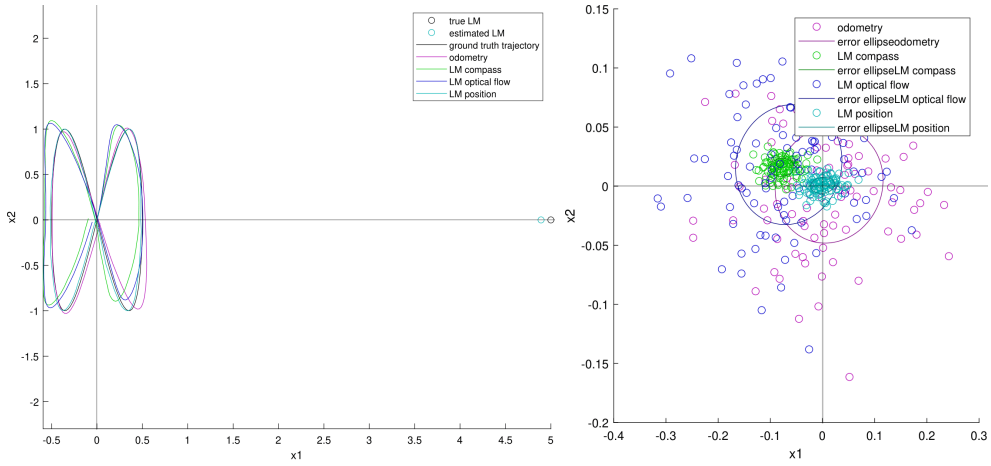

Figure 6.10: The estimated trajectories (left) are shown as well as the final position error (right) with the following parameters: Trajectory: loop, additive error: 0.025, multiplicative error: 0.025, landmark distance: 5

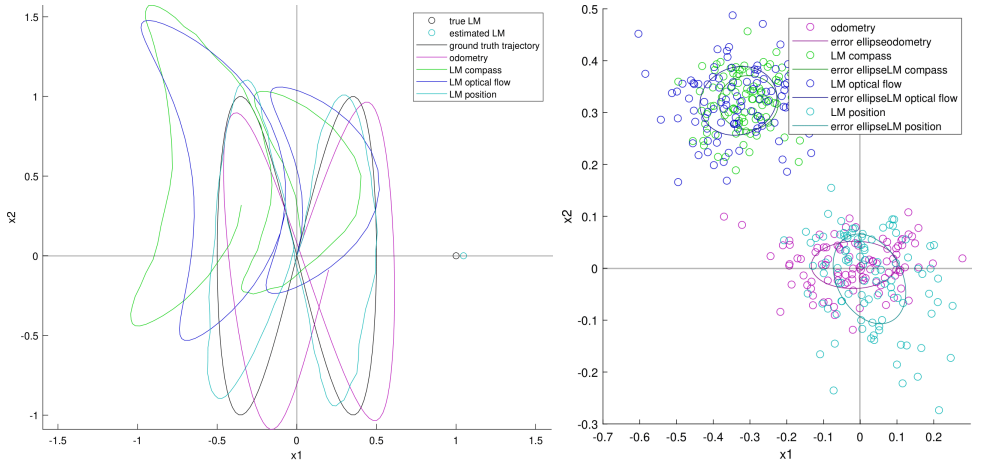

Figure 6.11: The estimated trajectories (left) are shown as well as the final position error (right) with the following parameters: Trajectory: loop, additive error: 0, multiplicative error: 0.1, landmark distance: 1

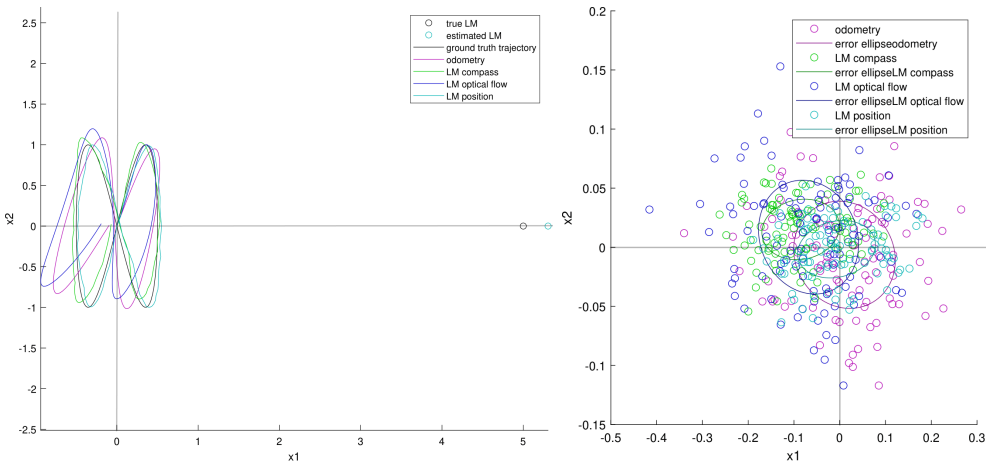

Figure 6.12: The estimated trajectories (left) are shown as well as the final position error (right) with the following parameters: Trajectory: loop, additive error: 0, multiplicative error: 0.1, landmark distance: 5

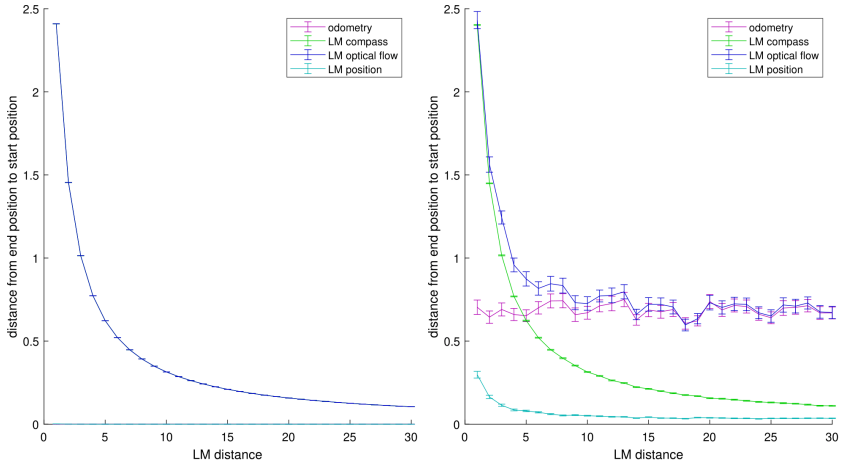

Figure 6.13: The distance error relative to the landmark position is shown with the following parameters: Trajectory: circle, additive error: 0 (left)/0.1 (right), multiplicative error: 0

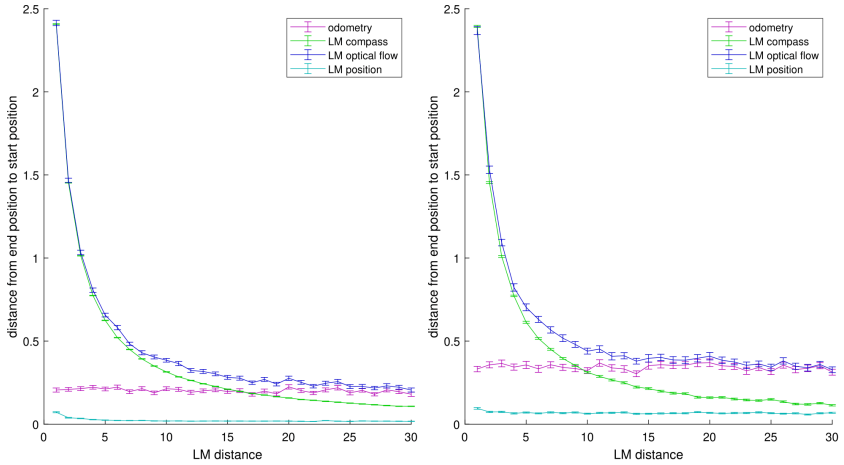

Figure 6.14: The distance error relative to the landmark position is shown with the following parameters: Trajectory: circle, additive error: 0.025 (left)/0 (right), multiplicative error: 0.025 (left)/0.1 (right)

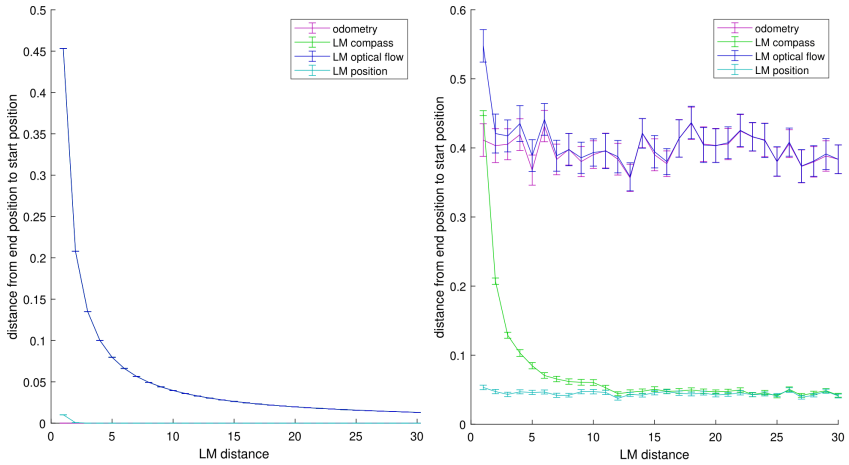

Figure 6.15: The distance error relative to the landmark position is shown with the following parameters: Trajectory: loop, additive error: 0 (left)/0.1 (right), multiplicative error: 0

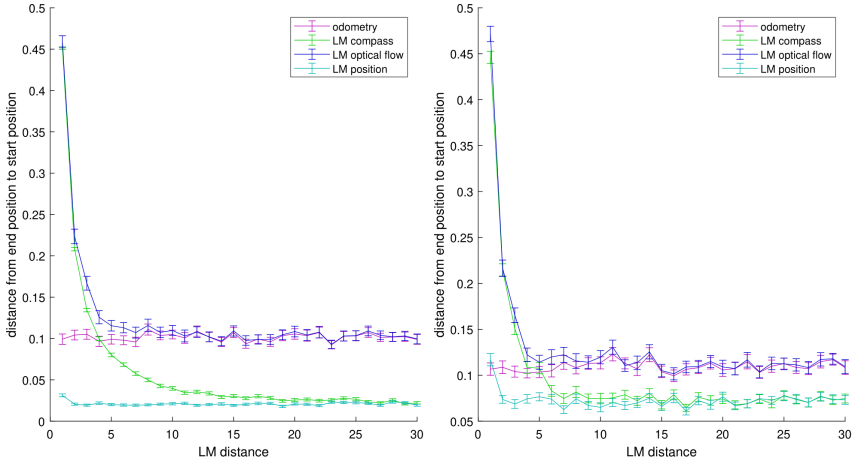

Figure 6.16: The distance error relative to the landmark position is shown with the following parameters: Trajectory: loop, additive error: 0.025 (left)/0 (right), multiplicative error: 0.025 (left)/0.1 (right)

List of Figures

References

Anagnostou, E., Skarlatou, V., Mergner, T., & Anastasopoulos, D. (2018, 09). Idiothetic signal processing and spatial orientation in patients with unilateral hippocampal sclerosis. *Journal of neurophysiology*, *120*, 1256-1263. doi: 10.1152/jn.00016.2018

Bailey, T., & Durrant-Whyte, H. (2006). Simultaneous localization and mapping (slam): part ii. *IEEE Robotics & Automation Magazine*, *13*, 108-117.

Cartwright, B., & Collett, T. (1983, 01). Landmark learning in bees. j comp physiol a. *Journal of Comparative Physiology*, *151*, 521-543. doi: 10.1007/BF00605469

Cheung, A., & Vickerstaff, R. (2010, 11). Finding the way with a noisy brain. *PLoS computational biology*, *6*, e1000992. doi: 10.1371/journal.pcbi.1000992

Etienne, A. S., Maurer, R., & Séguinot, V. (1996). Path integration in mammals and its interaction with visual landmarks. *Journal of experimental Biology*, *199*(1), 201-209. Retrieved from `https://archive-ouverte.unige.ch/unige:5684` (ID: unige:5684)

Gibson, J. J. (1950). *Perception of the Visual World*. Boston: Houghton Mifflin.

Gould, J. L. (2008). Animal navigation: The evolution of magnetic orientation. *Current Biology*, *18*(11), R482-R484. Retrieved from `https://www.sciencedirect.com/science/article/pii/S0960982208003941` doi: https://doi.org/10.1016/j.cub.2008.03.052

Klatzky, R. L., Loomis, J. M., Beall, A. C., Chance, S. S., & Golledge, R. G. (1998). Spatial updating of self-position and orientation during real, imagined, and virtual locomotion. *Psychological Science*, *9*(4), 293-298. Retrieved from `https://doi.org/10.1111/1467-9280.00058` doi: 10.1111/1467-9280.00058

Kurazume, R., & Hirose, S. (2000, January 1). An experimental study of a cooperative positioning system. *Autonomous Robots*, *8*(1), 43–52. doi: 10.1023/A:1008988801987

Papi, F. (1992). *Animal homing*. London: Chapman and Hall.

Steck, S. D., & Mallot, H. A. (2000). The role of global and local landmarks in virtual environment navigation. *Presence. Teleoperators and Virtual Environments*, *9*, 69-83.

Tinbergen, N., & Kruyt, W. (1938, 01). Über die orientierung des bienenwolfes (philanthus triangulum fabr.). *Zeitschrift für vergleichende Physiologie*, *25*, 292-334. doi: 10.1007/BF00339640

Urzua, S., Munguía, R., & Grau, A. (2017). Vision-based slam system for mavs in gps-denied environments. *International Journal of Micro Air Vehicles*, *9*(4), 283-296. Retrieved from `https://doi.org/10.1177/1756829317705325` doi: 10.1177/1756829317705325

Velik, R. (2008, 01). A model for multimodal humanlike perception based on modular hierarchical symbolic information processing, knowledge integration, and learning. In (p. 168 - 175). doi: 10.1109/BIMNICS.2007.4610105

Wang, K., Liu, Y., & Li, L. (2014). A simple and parallel algorithm for real-time robot localization by fusing monocular vision and odometry/ahrs sensors. *IEEE/ASME Transactions on Mechatronics*, *19*(4), 1447-1457. doi: 10.1109/TMECH.2014.2298247

Warren, W., & Hannon, D. (1988). Direction of self-motion is perceived from optical flow. *Nature*, *336*, 162-163.

Wiltschko, W., & Wiltschko, R. (2005, 09). Magnetic orientation and magnetoreception in birds and other animals. *Journal of comparative physiology. A, Neuroethology, sensory, neural, and behavioral physiology*, *191*, 675-93. doi: 10.1007/s00359-005-0627-7

Wolbers, T., Hegarty, M., B"uchel, C., & Loomis., J. M. (2008). Spatial updating: how the brain keeps track of changing object locations during observer motion. *Nature Neuroscience*, *11*, 1223-1230.

Yesiltepe, D., Dalton, R., Torun, A., Noble, S., Dalton, N., Hornberger, M., & Spiers, H. (2020, August 25). Redefining global and local landmarks: When does a landmark stop being local and become a global one? In J. Skilters, N. Newcombe, & D. Uttal (Eds.), *Spatial cognition - 12th international conference, spatial cognition 2020, proceedings* (pp. 111–121). Germany: Springer. doi: 10.1007/978-3-030-57983-8_9

Acknowledgement

I would like to thank Professor Dr. Mallot and Mr. Baumann for both their helpful support and their constructive suggestions during the supervision period. This has always helped me to orientate this exploratory work.
I would also like to thank my family and friends who have supported me during the last few months with motivation as well as proofreading.

Selbstständigkeitserklärung

Hiermit versichere ich, dass ich die vorliegende Bachelorarbeit selbstständig und nur mit den angegebenen Hilfsmitteln angefertigt habe und dass alle Stellen, die dem Wortlaut oder dem Sinne nach anderen Werken entnommen sind, durch Angaben von Quellen als Entlehnung kenntlich gemacht worden sind. Diese Bachelorarbeit wurde in gleicher oder ähnlicher Form in keinem anderen Studiengang als Prüfungsleistung vorgelegt.

Ort, Datum Unterschrift